Kunihisa Kozawa
Gunma Prefectural Institute of Public Health and Environmental Sciences, 378 Kamioki-machi, Maebashi-shi, Gunma 371-0052, Japan

Hirokazu Kimura*
Infectious Diseases Surveillance Center, National Institute of Infectious Diseases, 4-7-1 Gakuen, Musashimurayama-shi, Tokyo 208-0011, Japan
E-mail address: kimhiro@nih.go.jp

*Corresponding author. Tel.: +81 42 561 0771; fax: +81 42 565 3315.

Accepted 15 October 2012

http://dx.doi.org/10.1016/j.jinf.2012.10.022

Epidemiology and prognostic determinants of bacteremic acute pyelonephritis in women

To the Editor,

Lee and colleagues recently reported in this Journal the impact of discordant empirical therapy on outcome of community-acquired bacteremic acute pyelonephritis (APN).[1] APN is one of the most common infectious diseases.[2] The Infectious Diseases Society of America (IDSA) recommended fluoroquinolones as initial empiric therapy for APN where the frequency of resistance of community uropathogens to trimethoprim-sulfamethoxazole exceeds 20% and that to fluoroquinolones is less than 10%.[3] Hence concern about inappropriate empirical therapy for bacteremic APN has arisen.[1] The aim of this study was to determine the epidemiology of bacteremic APN in women during 1991–2010 in our setting and to identify the independent prognostic factors of mortality in these cases.

The setting was the Hospital Clínic in Barcelona, Spain. This hospital has followed a blood culture surveillance programme since 1991. Briefly, an infectious disease specialist and one microbiologist review the charts of patients with positive blood cultures and recommend antibiotic therapy according to the clinical context and the results of the Gram's stain organism identification and antimicrobial susceptibility test. Patients were observed from the diagnosis of bacteraemia until 30 days afterwards, until death in hospital or until discharge.

The type of study was based on an analysis of women with bacteraemia due to APN prospectively collected through the previously described blood culture surveillance programme from January 1991 to December 2010. Patients with bacteraemia due to UTI and urinary catheter or past urogenital surgery including all surgeries that resulted in anatomical alteration (egg, nephrectomy, neobladder formation and resection) were excluded. The Ethics Committee of the hospital approved the study.

APN was diagnosed with the simultaneous presence of (in the absence of another focus) (1) fever of over 38 °C as an axillary temperature or systemic inflammatory response syndrome; (2) pyuria, defined as the presence of 5 or more leukocytes per high-power field of urinary sediment or positive urine culture; other clinical signs that may be present are: dysuria syndrome (painful urination, sense of residual urine, or urinary frequency) and tenderness in the flank.

Significant bacteraemia was defined as one or more blood cultures positive for one or more primary pathogen and clinically apparent signs and symptoms of sepsis.[4] The origin of bloodstream infections was considered as: 1) nosocomial when cultures of blood specimens obtained >48 h after admission were positive; 2) community-acquired when cultures were obtained prior to admission or during the first 48 h without hospitalization or healthcare contact during the month before bacteraemia, and 3) healthcare-related when there was hospitalization or healthcare contact during the month before bacteraemia. For analysis purposes we divided the origin of bacteraemia into two categories: community-acquired and healthcare-associated (this included nosocomial and healthcare-related).[5] The prognosis of the underlying disease was classified, according to the criteria of McCabe and Jackson, as rapidly fatal (when death was expected within ≤3 months), ultimately fatal (when death was expected within a period of >3 months but <5 years) and non-fatal (when life expectancy was ≥5 years).[6] Prior antibiotic therapy was defined as the use of any antimicrobial agent for ≥3 days during the month prior to the occurrence of the bacteremic episode. Antibiotic treatment, either empirical or definitive (before or after the microbiological results and susceptibilities were known, respectively), was considered appropriate if at least one of the antibiotics involved had *in vitro* activity against the bacteria and the dose and route of administration were adequate. Shock was defined as a systolic pressure of <90 mmHg that was unresponsive to fluid treatment or required vasoactive drug therapy.[4] Death was considered related to the bloodstream infection if it occurred before the resolution of symptoms or signs or within 7 days of the onset of bacteraemia, and if there was no other explanation; otherwise, death within 30 days of the beginning of bacteraemia was considered unrelated to the episode.

Statistical analyses were carried out using the program SPSS (version 16.0; SPSS, Chicago, IL, USA). For analysis purposes, we considered related and unrelated mortality (within 30 days of bloodstream infection) together.

APN was the confirmed source of 2238 women with bacteraemia identified along the period of study 1991–2010. The mean age was 65 yr (SD: 20). Diabetes mellitus and solid-organ cancer were the most frequent underlying comorbidities. 1985 (89%) cases were community-acquired. There were 210 (9%) cases with shock on presentation and mortality accounted for 85 cases (4%).

Microbiological results are summarized in Table 1. The most common microorganisms isolated were *Escherichia coli*, *Klebsiella* spp. and *Proteus mirabilis* and their frequency remained stable throughout the years of study. There were 414 (18%) antibiotic-resistant (fluoroquinolone or cefotaxime) *E. coli* and *Klebsiella* spp. (AREK) isolates.

PLOS | ONE

Molecular Evolution of Hemagglutinin (*H*) Gene in Measles Virus Genotypes D3, D5, D9, and H1

Mika Saitoh,
Makoto Takeda,
Koichi Gotoh,
Fumihiko Takeuchi,
Tsuyoshi Sekizuka,
Makoto Kuroda,
Katsumi Mizuta,
Akihide Ryo,
Ryota Tanaka,
Haruyuki Ishii,
Hayato Takada,
Kunihisa Kozawa,
Ayako Yoshida,
Masahiro Noda,
Nobuhiko Okabe,
Hirokazu Kimura

Abstract

We studied the molecular evolution of *H* gene in four prevalent Asian genotypes (D3, D5, D9, and H1) of measles virus (MeV). We estimated the evolutionary time scale of the gene by the Bayesian Markov Chain Monte Carlo (MCMC) method. In addition, we predicted the changes in structure of H protein due to selective pressures. The phylogenetic tree showed that the first division of these genotypes occurred around 1931, and further division of each type in the 1960–1970s resulted in four genotypes. The rate of molecular evolution was relatively slow (5.57×10^{-4} substitutions per site per year). Only two positively selected sites (F476L and Q575K) were identified in H protein, although these substitutions might not have imparted significant changes to the structure of the protein or the epitopes for phylactic antibodies. The results suggested that the prevalent Asian MeV genotypes were generated over approximately 30–40 years and H protein was well conserved.

Citation: Saitoh M, Takeda M, Gotoh K, Takeuchi F, Sekizuka T, et al. (2012) Molecular Evolution of Hemagglutinin (*H*) Gene in Measles Virus Genotypes D3, D5, D9, and H1. PLoS ONE 7(11): e50660. doi:10.1371/journal.pone.0050660

Editor: Paul J. Planet, Columbia University, United States of America

Received: May 18, 2012; **Accepted:** October 25, 2012; **Published:** November 29, 2012

Funding: No current external funding sources for this study.

Competing interests: The authors have declared that no competing interests exist.

Introduction

Measles virus (MeV) of genus *Morbillivirus* and family *Paramyxoviridae* causes acute and highly contagious measles infection in humans [1], [2]. Since the year 2000, the number of patients in many countries with measles has continued to decrease due to widespread measles immunization programs [3]. Nevertheless, an estimated 300,000 cases were reported and 140,000 young children died from measles globally in 2010 (Media Centre. Measles. World Health Organization. http://www.who.int/mediacentre/factsheets/fs286/en/index.html). Thus, the World Health Organization has focused on the infection as an eliminative disease.

Many genotypes of MeV have been identified, although the virus may be confirmed as a monoserotype [1], [2]. Interestingly, there are associations between the prevalence of each genotype and geographical area [4]. For example, genotypes D4 and D6 are mainly detected in European countries, while genotypes D3, D5, D9, and H1 are mainly detected in Asian countries [4]. At present, in some countries that have eliminated measles, a small numbers of cases are caused by a number of different genotypes that reflect various sources of imported viruses [2]. The MeV genome encodes some essential structural proteins such as hemagglutinin (H) and fusion (F) proteins [1]. The H protein generally regulates viral adsorption and entry, and that of the vaccine strains shows hemagglutinin activity as well [1]. The neutralizing antibodies against H protein act as protective antibodies in MeV infection. In addition, recent studies have shown the detailed structure of the H protein and the epitopes for the neutralizing antibodies [5], [6]. Such antigenic changes may occur through positively selected amino acid substitutions due to selection pressures in the host. Indeed, attachment glycoprotein (G protein), an essential antigen of respiratory syncytial virus, shows frequent positive selections in the epitopes of the protein, whereas no positive selection sites have been found in the HN protein (a major antigen) of human parainfluenza virus type 1 [7], [8]. This suggests that the frequency of the positive selection sites differs among the major antigens of these viruses, even though the viruses all belong to the same family, *Paramyxoviridae*. Thus, it may be important to analyze the molecular evolution of *H* gene in MeV.

The Bayesian Markov Chain Monte Carlo (MCMC) method enables the evolutionary time scale to be estimated [9], [10]. Furthermore, detailed changes in H protein structure may be predictive. In the present study we conducted a detailed genetic analysis of the gene and predicted changes in the structure of H protein to gain a better understanding of the evolution of *H* gene in prevalent Asian MeV genotypes (D3, D5, D9, and H1).

Results

Phylogenetic Analysis Using the Bayesian MCMC Method on the *H* Coding Region of MeV

The phylogenetic tree constructed using the Bayesian MCMC method with the nucleotide sequences of the *H* gene (1854 nt) for various genotypes (A to H) of MeV is

shown in Fig. 1. The year of the first major division in the present tree was estimated as approximately 1931 (95% confidence interval [CI] 1906–1952). The D3, D5, and D9 subdivisions occurred in approximately 1975 (95% CI 1970–1980) and 1977 (95% CI 1972–1982), and the H1 and H2 subdivisions occurred in approximately 1966 (95% CI 1950–1979), resulting in the formation of 4 genotype clusters [D3 (14 strains), D5 (14 strains), D9 (6 strains), and H1 (27 strains)]. Further division of each genotype occurred in approximately 1980 (95% CI 1976–1983) for D3, 1980 (95% CI 1974–1985) for D5, 1987 (95% CI 1980–1993) for D9, and 1977 (95% CI 1968–1984) for H1. The CIs for each node of the phylogenetic tree are expressed as gray bars in Fig. 1. The rate of molecular evolution was estimated from the tree as 5.57×10^{-4} substitutions per site per year (95% CI 4.50×10^{-4}–6.81×10^{-4}).

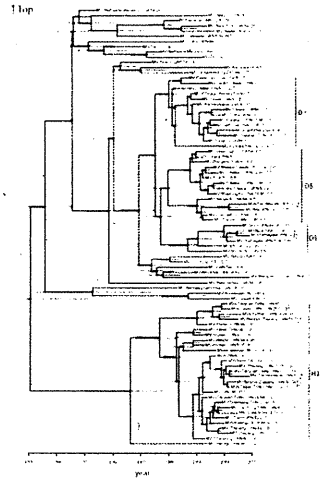

Figure 1. Phylogenetic tree of *H* gene by Bayesian Markov Chain Monte Carlo (MCMC) method.
The MCMC tree was based on the full nucleotide sequence of *H* gene (1854 nt) visualized in FigTree. The branch length reflects the evolutionary rate of individual sequences and their reconstructed ancestors. Gray bars indicate 95% confidence intervals for the estimated year. MeV strains were named according to WHO standard nomenclature. The strain names provide following information. MVi: sequence derived from RNA extracted from measles virus isolate in cell culture, MVs: sequence derived from RNA extracted from clinical material/city or province and country: use ISO-3 letter designation/date of onset of rash by epidemiological week and year, and isolate or sequence numbers/genotype in square brackets.
doi:10.1371/journal.pone.0050660.g001

Analysis of Selective Pressure of *H* Gene in MeV

Selection pressure analysis was performed in the strains of the various genotypes (A to H) in MeV *H* gene, and dN/dS values were calculated by the single likelihood ancestor counting (SLAC), fixed effects likelihood (FEL), and internal fixed effects likelihood (IFEL) methods, significant at the $p<0.05$ level. The global estimate of dN/dS was 0.22 (95% CIs of 0.19–0.24) by SLAC. Estimates of the dN/dS ratio of two codons were detected and two amino acid substitutions were estimated (F476L and Q575K) by the FEL and IFEL methods (Table 1). Negatively selected sites were detected by each of the three methods and 28 codons were identified (Table 1).

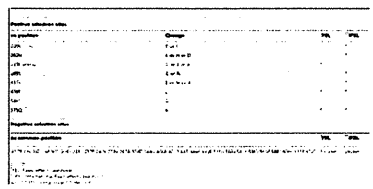

Table 1. Positive and negative selection sites in MeV H coding region in the present study.
doi:10.1371/journal.pone.0050660.t001

Location of the Two Positively Selected Amino Acid Sites

The two amino acid positions (476 and 575) were shown on the H protein structure [6]. The residues are exposed on the surface (light green and blue, respectively; Fig. 2). Therefore, they may be parts of epitopes, but to date there are no reports showing that the regions containing residues 476 or 575 constitute epitopes (known epitopes are shown in red in Fig. 2). The structural data showed that these residues are located at the bottom and lateral surfaces, respectively, of the H head dimer, and distal from the SLAM-binding site (SLAM is shown in cyan in Fig. 2).

Figure 2. The predicted structure of H protein in MeV.
The H head dimers are shown from the top, bottom, and lateral angles. Each monomer is shown in gray or orange. Residues reported to constitute epitopes are shown in red. SLAM is shown in cyan. Positively selected amino acid sites, 476 and 575, are shown in light green and blue, respectively.
doi:10.1371/journal.pone.0050660.g002

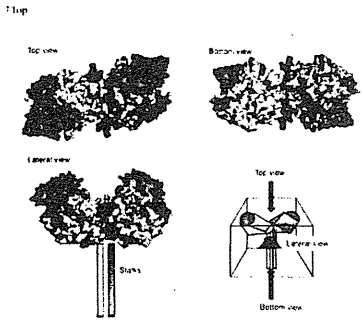

Discussion

We analyzed the molecular evolution of *H* gene in genotypes D3, D5, D9, and H1 of MeV, which are prevalent in Asian countries including China and Japan. First, we estimated the evolutionary time scale of the gene using the Bayesian MCMC method. The first division of these genotypes in the present tree was estimated as approximately 1931, and each genotype further divided in the 1960–70s, resulting in 4 genotypes. In addition, only two positively selected sites were observed, although these changes might not reflect significant structural changes in H protein. The results suggested that the 4 genotypes were formed over a period of approximately 30–40 years (from approximately 1931 to the 1960–70s) and the structure of the H protein has been well conserved.

MeV genotype D3 was mainly detected in various Western Pacific countries including Japan, Australia, Papua New Guinea, and the Philippines during 1983–2006, and was endemic in Papua New Guinea and possibly the Philippines from 2002–2006 [2], [11], [12]. The first major division of type D3 was estimated at around 1975, and the ancestral strains further subdivided from around 1980 (Fig. 1). Genotype D5 has been prevalent in Japan, Australia, and Cambodia since 1985 [2], [11], [12]. Until 2001, both D3 and the D5 genotypes were endemic in Japan. The first major division of type D5 was estimated at around 1975, and extensive branching into two clusters occurred around 1980. Furthermore, it is suggested that the ancestral strains have undergone further divisions from around 1990. Genotype D9 was first described after importation to Australia from Indonesia in 1999 and was associated with an outbreak in Japan in 2004 [2], [11], [12]. The strains detected in Japan and France in the mid-2000s had diverged in approximately 1990 from the strains detected in Australia in 1999. Genotype H1, detected during the large measles epidemic in Korea in 2000–2001, has been prevalent in China, Japan, Korea, Vietnam, and Australia since 1993 and is mainly associated with transmission within China or in importations from China [2], [11], [12]. This genotype diverged into plural clusters after 1977. The Korean strain detected in Korea in 2000 evolved from one Chinese strain clusters in about 1995. The results showed that the Asian prevalent MeV genotypes D3, D5, D9, and H1 were generated over approximately 30–40 years, and the ages of the diverged clusters for each genotype could be predicted. In the present study, it is estimated that each genotype, e.g., D3, D5, D9, and H1, was generated from the 1960s to 70s. However, there was a difference in the year that the viruses were generated according to the phylogenetic tree based on the Bayesian MCMC method and the year that they were first detected. For example, the D9 strain was shown to be generated approximately 40 years ago using the phylogenetic tree, while the virus was detected in 1999. This has been seen in other viruses, such as rubella virus [13]. Indeed, Zhu et al. showed that cluster 1 isolates of Chinese genotype 1E rubella virus were collected from 2001 to 2009, while the viruses were estimated to have appeared in 1997 according to the MCMC method. To solve this discrepancy, additional studies are needed.

We analyzed the rate of molecular evolution from the tree as 5.57×10^{-4} substitutions per site per year. The rates of evolution of *H* gene in seasonal influenza virus subtype A and *G* gene in respiratory syncytial virus are estimated at about 10^{-3} substitutions per site per year [14], [15]. In addition, we reported that the rate of *HN* gene in human parainfluenza virus type 1 is estimated at 7.68×10^{-4} substitutions/site/year [8]. These results suggest that the rate of evolution of *H* gene of MeV may be similar to the rate of *HN* gene of human parainfluenza virus type 1, and their rates of molecular evolution may be relatively slow [8].

We estimated positively and negatively selected sites in the gene by the SLAC, FEL, and IFEL methods. Positive selection shows a survival advantage under the selective constraints that confront the viral population [16]. Negative selection plays an important role in maintaining the long-term stability of biological structures by removing deleterious mutations [16], [17]. In this study, two positively selected sites (F476L and Q575K) were found. Woelk et al demonstrated 14 positively selected sites in 50 strains of *H* gene in all genotypes of MeV [18]. Of these, amino acid positions corresponding to 476 and 575 are compatible with our results. Region 463–477 including site 476 and region 561–575 including site 575 react with human sera. Furthermore, region 463–477 is a possible candidate for interaction with the CD46 receptor. In addition, Corey and Iorio have shown that amino acid substitutions at region 473–477 including 476 drastically reduce hemagglutinin activity associated with fusion promotion [19]. In this study, it is suggested that the amino acid substitutions of two positively selected sites share these particular abilities in MeV *H* gene. Twenty- eight negatively selected sites were found (Table 1). These sites may be optimized biological structures, thus further analysis of the biological properties of H glycoprotein in MeV is required. In addition, it may be important to make a distinction between the branched year of the viruses on a phylogenetic tree and the nucleotide and amino acid substitutions as positive selection. Although this question could not be elucidated in the present study, further studies regarding these relationships are needed.

Finally, we predicted the changes of the epitopes [5], [6] for neutralizing antibodies against H protein by substitutions of the amino acid due to positive selection pressure. The amino acid changes at positively selected sites may confer an advantage to MeV in terms of transmission. The residues at amino acid positions 476 and 575 are exposed on the surface, but are located distal from receptor binding site and unrelated to known neutralizing epitopes. Therefore, the amino acid substitutions at these positions may not significantly affect the efficacy of humoral immunity against MeV. These data suggested that in these several decades none of the amino acid substitutions on the epitopes succeeded to give MeV better fitness in nature significantly. These observations could provide a rationale for the high efficacy of currently used MeV vaccines against all MeV strains circulating. In conclusion, it suggested that the prevalent Asian MeV genotypes were generated over approximately 30–40 years and H protein was well conserved. As an essential molecule of these viruses, further analysis of the biological properties of H glycoprotein in MeV is required. Thus, additional and larger molecular epidemiological studies are required to give better understanding of the etiology of MeV.

Materials and Methods

Strains

We comprehensively collected total 162 strains of various genotypes of *H* gene sequence (1854 nt), such as 23 reference strains (genotypes A, B1 to B3, C1, C2, D1, D2, D4, D6 to D8, D10, D11, E, F, G1 to 3, and H2 [2]) and Asian-prevalent genotype strains, including the reference strains (D3, 37 strains; D5, 34 strains; D9. 11 strains; and H1, 57 strains), from MeaNS (http://www.hpa-bioinformatics.org.uk/Measles/Public/Web_Front/main.php) [20]. Their sequences correspond to positions 21–1874 (1854 nt) of MVi/Chicago.Illinois.USA/89 (reference strain for genotype D3) (GenBank accession number M81895). The MeV sequences were aligned using the ClustalW web server (http://www.ddbj.nig.ac.jp/index-j.html).

Phylogenetic Analysis by the Bayesian MCMC Method

Using all of the present strains to estimate the rate of molecular evolution (and hence a time scale) and evolutionary relationships, phylogenetic analyses were performed using the Bayesian MCMC method in the BEAST program (version 1.7.2) [21]. The time of the most recent common ancestor (tMRCA) with a 95% highest

posterior density (HPD) was estimated by Bayesian molecular dating as described previously [9], [10]. The MeV sequences were aligned using the ClustalW web server (http://www.ddbj.nig.ac.jp/index-j.html). We removed the identical sequences from within the MeV *H* coding region of the genotype strains. The dataset was analyzed under a lognormal relaxed uncorrelated clock using the general time reversible (GTR) model with the gamma distributed rates across sites (GTR+Γ) model selected by the KAKUSAN4 program (version 4.0). The MCMC chain was run for 30,000,000 steps and sampled every 1,000 steps. Uncertainty in the estimates was indicated by the 95% HPD intervals. The parameter outputs generated by the Bayesian MCMC runs and convergence on the basis of the effective sampling size after a 10% burn-in were analyzed using the TRACER program (version 1.5). The trees were summarized in a target tree using the Tree Annotator program (version 1.7.2) by choosing the tree with the maximum posterior probabilities after a 10% burn-in. The phylogenetic tree was viewed in FigTree (version 1.3.1; available at: http://beast.bio.ed.ac.uk). Next, to understand the phylogenetic tree easily, we selected and removed the sequences with high homogeneity and identical isolation years in each cluster of the tree. As a result, the present phylogenetic tree included 23 genotypes of the reference strains and the Asian-prevalent strains, including the reference strains (14 strains of D3, 14 strains of D5, 6 strains of D9, and 27 strains of H1).

Selective Pressures Analysis

To evaluate selective pressures on the *H* coding regions among all MeV strains, the rates of synonymous (dS) and non-synonymous (dN) changes at amino acid sites were estimated by conservative SLAC, FEL, and IFEL methods using ML available on the Datamonkey webserver (http://www.datamonkey.org/) [22]. The SLAC method is suitable for fast likelihood-based "counting methods" that employ either a single most likely ancestral reconstruction, weighted across all possible ancestral reconstructions, or sampling from ancestral reconstructions. The FEL method directly estimates dN and dS substitution rates at each site. The IFEL method is tested for only along internal branches of the phylogeny in the same manner. To examine the dN and dS rates, these methods were performed incorporating the GTR model of nucleotide substitution and the phylogenetic tree deduced using the NJ method. The dN/dS values of each codon and branch of the present phylogenetic tree were assessed as described previously [23]. Positive (dN>dS) and negative (dN<dS) selections were predicted using the *p*-value [23].

Prediction of Epitopes for Neutralizing Antibody Against MeV H Protein Based on the Deduced Amino Acid Substitutions

To clarify the location of substituted amino acids on the H protein, we mapped the positively and negatively selected sites as previously described [5], [6]. Figures were produced using PyMOL (DeLano Scientific LLC, Palo Alto, CA, USA. http://www.pymol.org.).

Author Contributions

Conceived and designed the experiments: HK MT. Performed the experiments: MS HK KG KM AY MN. Analyzed the data: AR RT HI HT KK NO. Contributed reagents/materials/analysis tools: FT TS MK. Wrote the paper: HK MS MT.

References

1. Griffin DE (2007) Measles viruses. In: Knipe DM, Howley PM, editors. Fields virology. 5th ed. Vol. 2. Philadelphia: Lippincott Williams & Wilkins. 1551–1585.
2. Griffin DE, Oldstone MBA (2009) Measles: Pathogenesis and control. Berlin: Springer-Verlag. 292 p.
3. Centers for Disease Control and Prevention (CDC) (2012) Progress in global measles control, 2000–2010. MMWR Morb Mortal Wkly Rep 61: 73–78. Find this article online
4. World Health Organization (2006) Global distribution of measles and rubella genotypes-update. WER 81: 469–480. Find this article online
5. Hashiguchi T, Kajikawa M, Maita N, Takeda M, Kuroki K, et al. (2007) Crystal structure of measles virus hemagglutinin provides insight into effective vaccines. Proc Natl Acad Sci U S A 104: 19535–19540. doi: 10.1073/pnas.0707830104. Find this article online
6. Hashiguchi T, Ose T, Kubota M, Maita N, Kamishikiryo J, et al. (2011) Structure of the measles virus hemagglutinin bound to its cellular receptor SLAM. Nat Struct Mol Biol 18: 135–141. doi: 10.1038/nsmb.1969. Find this article online
7. Woelk CH, Holmes EC (2001) Variable immune-driven 415 natural selection in the attachment (G) glycoprotein of respiratory syncytial virus (RSV). J Mol Evol 52: 182–192. Find this article online
8. Mizuta K, Saitoh M, Kobayashi M, Tsukagoshi H, Aoki Y, et al. (2011) Detailed genetic analysis of hemagglutinin-neuraminidase glycoprotein gene in human parainfluenza virus type 1 isolates from patients with acute respiratory infection between 2002 and 2009 in Yamagata prefecture, Japan. Virol J 8: 533. doi: 10.1186/1743-422X-8-533. Find this article online
9. Thorne JL, Kishino H, Painter IS (1998) Estimating the rate of evolution of the rate of molecular evolution. Mol Biol Evol 15: 1647–1657. doi: 10.1093/oxfordjournals.molbev.a025892. Find this article online
10. Lepage T, Bryant D, Philippe H, Lartillot N (2007) A general comparison of relaxed molecular clock models. Mol Biol Evol 24: 2669–2680. doi: 10.1093/molbev/msm193. Find this article online
11. Riddell MA, Rota JS, Rota PA (2005) Review of the temporal and geographical distribution of measles virus genotypes in the prevaccine and postvaccine eras. Virol J 2: 87. Find this article online
12. World Health Organization (2010) Programmatic feasibility reports - per region and including comprehensive epidemiological data. WPRO: WPRO Feasibility Report. Available: http://www.who.int/immunization/sage/previous_november2010/en/index.html. Accessed: 2012 Feb 13.
13. Zhu Z, Cui A, Wang H, Zhang Y, Liu C, et al. (2012) Emergence and continuous evolution of genotype 1E Rubella viruses in China. J Clin Microbiol 50: 353–363. doi: 10.1128/JCM.01264-11. Find this article online
14. Yoshida A, Kiyota N, Kobayashi M, Nishimura K, Tsutsui R, et al. (2012) Molecular epidemiology of attachment glycoprotein (G) gene in respiratory syncytial virus in children with acute respiratory infection in Japan in 2009/2010. J Med Microbiol. In press.
15. Webster RG, Bean WJ, Gorman OT, Chambers TM, Kawaoka Y (1992) Evolution and ecology of influenza A viruses. Microbiol Rev 56: 152–179. Find this article online
16. Domingo E (2007) Virus evolution. In: Knipe DM, Howley PM, editors. Fields virology. 5th ed. Vol. 2. Philadelphia: Lippincott Williams & Wilkins. 389–421.
17. Loewe L (2008) Negative selection. Nature Education: 1.
18. Woelk CH, Jin L, Holmes EC, Brown DW (2001) Immune and artificial selection in the haemagglutinin (H) glycoprotein of measles virus. J Gen Virol 82: 2463–2474. Find this article online
19. Corey EA, Iorio RM (2009) Measles virus attachment proteins with impaired ability to bind CD46 interact more efficiently with the homologous fusion protein. Virology 383: 1–5. doi: 10.1016/j.virol.2008.10.018. Find this article online
20. World Health Organization (2012) Measles virus nomenclature update: 2012. WER 87: 73–80. Find this article online
21. Drummond AJ, Rambaut A (2007) BEAST: Bayesian evolutionary analysis by sampling trees. BMC Evol Biol 7: 214. doi: 10.1186/1471-2148-7-214. Find this article online
22. Pond SL, Frost SD (2005) Datamonkey: Rapid detection of selective pressure on individual sites of codon alignments. Bioinformatics 21: 2531–2533. doi: 10.1093/bioinformatics/bti320. Find this article online
23. dos Reis M, Yang Z (2011) Approximate likelihood calculation on a phylogeny for Bayesian estimation of divergence times. Mol Biol Evol 28: 2161–2172. doi: 10.1093/molbev/msr045. Find this article online

Microbiology and Immunology

Microbiol Immunol 2012; **56**: 855–858
doi:10.1111/j.1348-0421.2012.00507.x

NOTE

Epidemiology of parainfluenza virus types 1, 2 and 3 infections based on virus isolation between 2002 and 2011 in Yamagata, Japan

Katsumi Mizuta[1], Chieko Abiko[1], Yoko Aoki[1], Tatsuya Ikeda[1], Tsutomu Itagaki[2], Fumio Katsushima[3], Yuriko Katsushima[3], Yoko Matsuzaki[4], Masahiro Noda[5], Hirokazu Kimura[5] and Tadayuki Ahiko[1]

[1]Department of Microbiology, Yamagata Prefectural Institute of Public Health, Yamagata, Yamagata 990-0031, [2]Yamanobe Pediatric Clinic, Yamanobe, Yamagata 990-0301, [3]Katsushima Pediatric Clinic, Yamagata, Yamagata 990-2461, [4]Department of Infectious Diseases, Yamagata University Faculty of Medicine, Yamagata, Yamagata 990-9585, and [5]Infectious Diseases Surveillance Center, National Institute of Infectious Diseases, 4-7-1, Gakuen, Musashimurayama, Tokyo 208-0011, Japan

ABSTRACT

To clarify the epidemiology of viral acute respiratory infections (ARIs), 305 human parainfluenza virus types 1 (HPIV1), 154 HPIV2 and 574 HPIV3 strains were isolated from 16,962 nasopharyngeal swabs obtained between 2002 and 2011 at pediatric clinics in Yamagata, Japan. The total isolation frequency for HPIV1–3 was 6.1%. Unlike HPIV1 infections, HPIV3 showed clear seasonality with yearly outbreaks in the spring–summer season. HPIV2 tended to appear biannually in autumn–winter. Although no reliable techniques for the laboratory diagnosis of these infections have been established, the present results suggest that HPIV1–3 are an important causative agent of ARIs in children.

Key words acute respiratory infection, epidemiology, parainfluenza, seasonality.

Human parainfluenza viruses are enveloped, negative-sense RNA viruses that belong to the family *Paramyxoviridae* (1, 2). There are four genetically different types: HPIV1 to HPIV4; HPIV1 and HPIV3 belong to the genus *Respirovirus* and HPIV2 and HPIV4 to the genus *Rubulavirus* (1, 2). Although HPIV4 is rarely reported, HPIV1–3 are important causes of various ARIs in children, including the common cold, croup, bronchitis, bronchiolitis, and pneumonia. They also commonly reinfect older children and adults. Although such infections are generally mild in healthy persons, they can cause serious disease in immunocompromised hosts (3). In Japan, fewer HPIV strains have been detected than have strains of other respiratory viruses, such as RSV (4). There have been few epidemiological studies and negligible data collected on HPIVs in Japan (5–8). Herein, we describe the results of virus isolation from patients with ARIs in Yamagata, Japan between 2002 and 2011, with particular focus on HPIVs.

In collaboration with the Yamagata prefectural health authorities for the national surveillance of viral diseases in Japan, between January 2002 and December 2011 we collected 16,962 nasopharyngeal swab specimens from patients with ARI attending two pediatric clinics (Yamanobe and Katsushima Pediatric Clinics). Among these specimens, 12,189 (71.9%) were from patients $\leq$5 years old, 2763 (16.3%) from patients between 6 and 9, 1466 (8.6%) from patients between 10 and 14, and 469 (2.8%) from patients $\geq$14. We placed the nasopharyngeal specimens in tubes containing 3 mL of transport medium and transported them to the Department of Microbiology, Yamagata Prefectural Institute of Public Health for virus isolation (9).

Correspondence
Katsumi Mizuta, Department of Microbiology, Yamagata Prefectural Institute of Public Health, Tokamachi 1-6-6, Yamagata, Yamagata 990-0031 Japan. Tel: +81 23 627 1373; Fax:+81 23 641 7486; e-mail: mizutak@pref.yamagata.jp

Received 19 July 2012; revised 20 August 2012; accepted 29 August 2012.

List of Abbreviations: ARI, acute respiratory infection; CPE, cytopathic effect; NESID, National Epidemiological Surveillance of Infectious Diseases; HMV-II, human malignant melanoma; HPIV, human parainfluenza virus; RSV, respiratory syncytial virus; RT, reverse transcription.

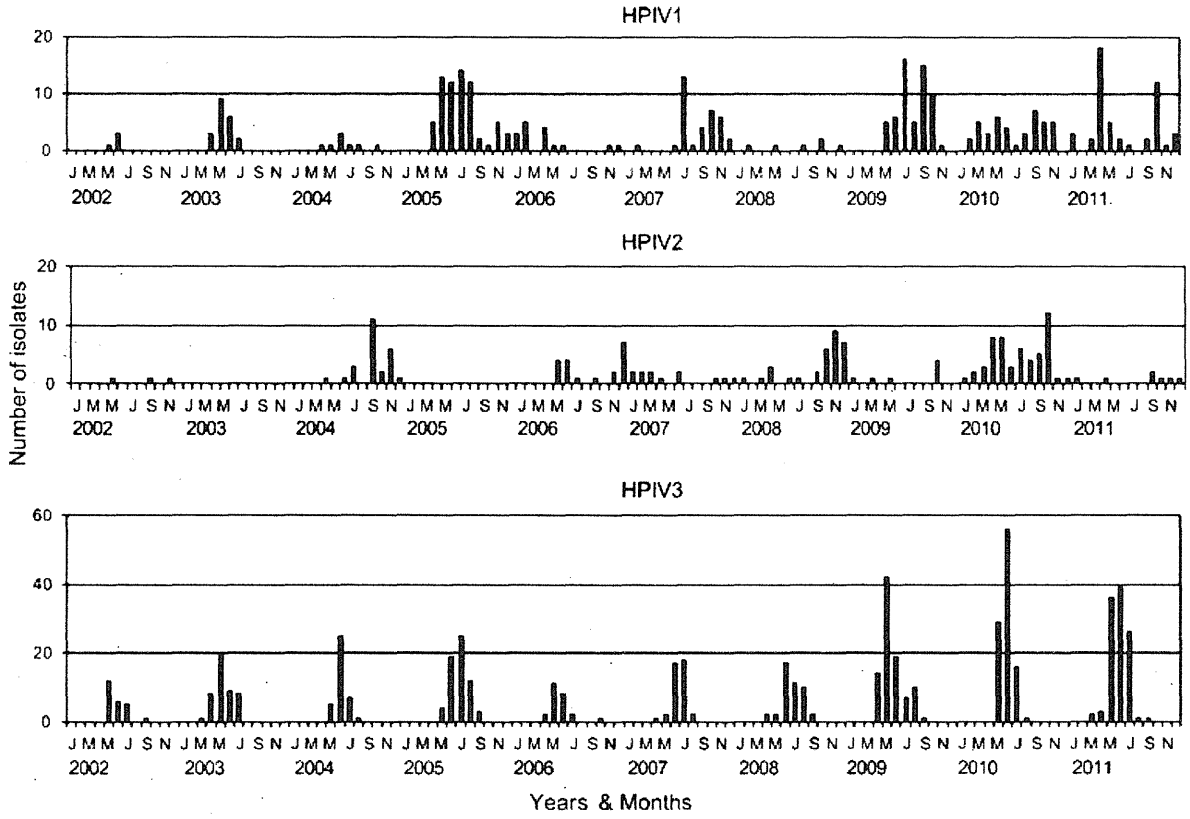

Fig. 1. Monthly distribution of human parainfluenza virus types 1-3 strains isolated from patients with acute respiratory infections in Yamagata, Japan between 2002 and 2011.

We have used HHVMRG plates, the acronym being derived from the human embryonic lung fibroblast (HEF), human laryngeal carcinoma (HEp-2), Vero, Madin Darby canine kidney (MDCK), rhabdomyosarcoma (RD-18S), and green monkey kidney (GMK) cell lines that they include, for virus isolation since June 2001 (10) and the HHVe6MRG plate, in which we substituted the VeroE6 cell line for the Vero cell line, since January, 2004 (9, 11). We used 96-well tissue culture plates (Greiner Bio-one, Frickenhausen, Germany) vertically and prepared two rows of each cell line as described previously (9, 11). Beginning in 2008, we also prepared HMV-II cell lines as separate 96-well tissue culture plates and inoculated the specimens onto them, mainly to isolate HPIVs (12, 13). After centrifugation of the specimens at 1500*g* for 20min, we inoculated 75μL of supernatant directly into two wells of each cell line. We stored the remainder of each specimen at −80C. We centrifuged the inoculated plates at 450*g* for 20min, incubated them at 33C in a 5% CO_2 incubator and assessed them for CPE for 14 days, except for the Vero E6 cell lines, which we observed for approximately one month without changing the medium to isolate human metapneumovirus (11).

When we observed a CPE or hemagglutination test and/or found a hemadsorption test to be positive using guinea pig erythrocytes (0.8%), we performed virus identification using a hemadsorption inhibition test, RT-PCR and sequence analysis as described previously (9, 12).

With regard to HPIVs, we isolated 1033 (6.1%) HPIV1–3 strains, comprising 305 HPIV1 (1.8%), 154 HPIV2 (0.9%) and 574 HPIV3 (3.4%) strains, from the 16,962 specimens we obtained during the study period. After we introduced the HMV-II cell line, the annual virus isolation frequencies of HPIV1–3 increased from 1.6 to 7.9% between 2002 and 2008 and from 9.4 to 10.8% between 2009 and 2011. Figure 1 shows monthly numbers of HPIV1–3 isolates. HPIV1 was uncommon in winter but quite commonly isolated between April and October. Further, although we isolated HPIV2 year-round, we recovered 55% of isolates between September and December. For HPIV3, we recovered 86% of isolates between May and July, but none between November and February, indicating that

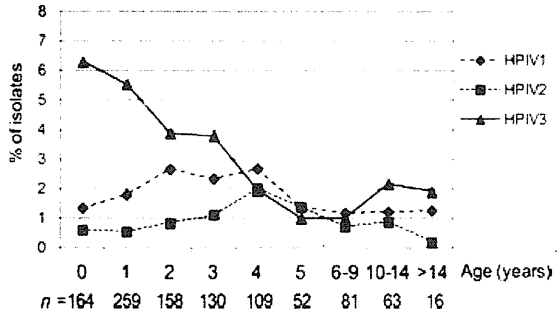

Fig. 2. Proportion of human parainfluenza types 1–3 isolated by age in patients with acute respiratory infections in Yamagata, Japan between 2002 and 2011.

HPIV3 infections have clear seasonality. Figure 2 shows a breakdown of HPIV1–3 infections by age. For HPIV3, 53.5% of the children were younger than 2 years and the proportion decreased with age apart from the ≥10 years age group. In contrast, we found the highest percentage of HPIV1 and HPIV2 infections in the 2–4 years (2.4–2.7%) and 3–5 years (1.1–2.0%) age groups, after which the percentage of infections generally decreased with age. Regarding the clinical diagnosis of patients with HPIV1, HPIV2 and HPIV3 infections, 236 (77.4%), 123 (79.9%), and 458 patients (79.8%) were diagnosed with upper respiratory infections such as rhino-pharyngitis, respectively; 25 (8.2%), 11 (7.1%), and 13 (2.3%) with croup, respectively; 32 (10.5%), 18 (11.7%), and 63 (11.0%) with lower respiratory infections such as bronchitis, bronchiolitis, and pneumonia; and the rest with other diseases including viral exanthema.

Human parainfluenza virus infections follow both endemic and epidemic patterns (1, 3); therefore, the seasonality of HPIVs varies depending on place, distinct variations being observed from year to year. The number of isolates of various viruses detected in public health laboratories all over Japan is available in the Infectious Agents Surveillance Report, Japan, for each year since 1981, the data between 1980 and 1991 being documented in published supplements (7, 8). All annual data are available from the NESID system (14). This NESID system database includes the data from Yamagata described in this study.

Several previous studies have reported that HPIV1 infections have clear outbreaks in autumn, mostly in September and November, either every two years (15–18) or at irregular intervals (19). In this study, we found no clear seasonality for HPIV1 infections, although HPIV1 infections did appear to be more common in odd-numbered years. In Japan, no source, including the NESID system, has indicated a seasonal pattern in HPIV1 infections (5–8, 14).

In comparison to the clear seasonality of HPIV1 and HPIV3 outbreaks, smaller yearly or irregular outbreaks of HPIV2 have reportedly occurred in autumn (15–19). In this study, we recovered many HPIV2 isolates in the autumn-winter season, observing a particular increase in even-numbered years since 2004 in Yamagata, Japan. The NESID system data support this trend: in the years prior to 1986, HPIV2 infections occurred more commonly in even-numbered years, apart from 1981 and 1983 (7, 8, 14). Thus, HPIV2 infections have commonly occurred in the autumn-winter season every two years in Japan, although this seasonality is less clearly observable than that of HPIV3.

In this study from 2002 to 2011 in Yamagata, Japan, we found HPIV3 infections to be grouped in clear yearly seasonal outbreaks, mainly between May and July. The data in the NESID system also show that HPIV3 infections have peaked in the spring-summer season since 1980 (7, 8, 14). Many previous studies have reported that HPIV3 causes yearly outbreaks, mainly in the spring-summer season, around the globe (15–20); the clear seasonality of HPIV3 in Yamagata appears similar to that observed in other areas.

It is generally accepted that HPIV3 as well as RSV infections are common in infants and young children, whereas HPIV1 and HPIV2 infections tend to be commoner in older persons (1–3, 15, 19). Knott *et al.* reported that the age distribution of HPIV3 infections peaks at 6 months–2 years of age, whereas HPIV1 and HPIV2 peak at 2–5 years (15): findings that are similar to our observations in this study. Clinically, fewer of our patients were diagnosed with croup (2.3–8.2%) than was reported by Knott *et al.* (9–45%) (15). However, both studies supported the contention that HPIV1 and HPIV2 are more strongly associated with croup than is HPIV3, which is in agreement with the trends described in various textbooks (1, 3).

This study indicates that the annual isolation frequencies of HPIV1–3 are 1.6–10.8%, and that those for HPIV1–3 infections are equal to or higher than those previously reported for RSV (2.2–3.2%) (9). However, in Japan fewer cases of HPIV1–3 than of RSV are detected: 1870 and 3462 cases were reported, respectively, between 2001 and 2010 (4). This could be because there is no established reliable technique for the laboratory diagnosis of HPIVs. Identification of the suspected causative agents and development of a system for their laboratory diagnosis are the first steps needed for the proper management and treatment of patients with infectious diseases. We hope this study will lead to a better understanding of the epidemiology and etiology of HPIVs and hopefully aid in the development of a rapid antigen test, such as immunochromatography, similar to those currently available for use in clinical settings

for influenza virus, adenovirus, RSV and human metapneumovirus.

ACKNOWLEDGMENTS

We thank the doctors, nurses and people of Yamagata Prefecture for their assistance and collaboration in the surveillance of viral infectious diseases. This work was partially supported by grants-in-aid from the Japan Society for Promotion of Science and for Research on Emerging and Re-emerging Infectious Diseases from the Ministry of Health, Labor and Welfare.

DISCLOSURE

All authors declare they have no conflicts of interests.

REFERENCES

1. Hodes D.S. (1992) Respiratory infections and sinusitis. In: Katz S.L., Gershon A.A., Hotez P.J. eds. *Krugman's Infectious Diesases of Children.* 10th edn. Missouri: Mosby-Year Book, pp 362–401.
2. Psarras S., Papadopoulos N.G., Johnston S.L. (2009) Parainfluenza viruses. In: Zukcerman A.J., Banatvala J.E., Schoub B.D., Griffiths P.D., Mortimer P. eds. *Principle & Practice of Clinical Virology.* 6th edn. West Sussex, UK: Wiley-Blackwell, pp 409–39.
3. Glezen W.P., Denny F.W. (1997) Parainfluenza viruses. In:Evans A.S., Kaslow R.A. eds. 4th edn. New York and London: Plenum Medical Book Company, pp 551–67.
4. Infectious agents surveillance report (IASR): Yearly reports of virus isolation/detection from human sources, 2001–2010, influenza and other respiratory viruses. http://idsc.nih.go.jp/iasr/virus/graph/infl01–10.pdf Accessed 27th June 2012.
5. Numazaki Y., Yano N., Shigeta S., Ikeda M., Takai S., Suto T., Ishida N. (1968) Studies on parainfluenza virus infections among infants and children in Sendai. II. Serologic and epidemiologic investigation. *Jpn J Microbiol* **12:** 343–51.
6. Numazaki Y., Ohshima T., Ohmi A., Tanaka A., Oizumi Y., Komatsu S., Takagi T., Karahashi M., Ishida N.(1987) A microplate method for isolation of viruses from infants and children with acute respiratory infections. *Microbiol Immunol* **31:** 1085–95.
7. Editorial committee of findings of infectious agents in Japan (1986) Summary of reported isolations of viruses, parainfluenza virus. *Jpn J Med Sci Biol* **39:** S48–49.
8. Editorial committee of findings of infectious agents in Japan (1992) Summary of reported isolations of viruses, parainfluenza virus. *Jpn J Med Sci Biol* **45:** S56–8.
9. Mizuta K., Abiko C., Aoki Y., Suto A., Hoshina H., Itagaki T., Katsushima N., Matsuzaki Y., Hongo S., Noda M., Kimura H., Ootani K. (2008) Analysis of monthly isolation of respiratory viruses from children by cell culture using a microplate method: a two-year study from 2004 to 2005 in Yamagata, Japan. *Jpn J Infect Dis* **61:** 196–201.
10. Mizuta K., Abiko C., Goto H., Murata T., Murayama S. (2003) Enterovirus isolation from children with acute respiratory infections and presumptive identification by a modified microplate method. *Int J Infect Dis* **7:** 138–42.
11. Abiko C., Mizuta K., Itagaki T., Katsushima N., Ito S., Matsuzaki Y., Okamoto M., Nishimura H., Aoki Y., Murata T., Hoshina H., Hongo S., Ootani K. (2007) Outbreak of human metapneumovirus detected by Vero E6 cell line in isolates collected in Yamagata, Japan between 2004 and 2005. *J Clin Microbiol* **45:**1912–9.
12. Mizuta K., Saitoh M., Kogayashi M., Tsukagoshi H., Aoki Y., Ikeda T., Abiko C., Katsushima N., Itagaki T., Noda M., Kozawa K., Ahiko T., Kimura H. (2011) Detailed genetic analysis of hemagglutinin-neuraminidase glycoprotein gene in human parainfluenza virus type 1 isolates from patients with acute respiratory infection between 2002 and 2009 in Yamagata prefecture, Japan. *Virology J* **8:** 533.
13. Moriuchi H., Oshima T, Nishimura H., Nakamura K., Katsushima N., Numazaki Y. (1990) Human malignant melanoma cell line (HMV-II) for isolation of influenza C and parainfluenza viruses. *J Clin Microbiol* **28:** 1147–50.
14. National Epidemiological Surveillance of Infectious Diseases (NESID) system: https://nesid3g.wish.mhlw.hq.admix.go.jp/ Accessed 27th June 2012.
15. Knott A.M., Long C.E., Hall C.B. (1994) Parainfluenza viral infections in pediatric outpatients: seasonal patterns and clinical characteristics. *Pediatr Infect Dis J* **13:** 269–73.
16. Hall C.B. (2001) Respiratory syncytial virus and parainfluenza virus. *N Engl J Med* **344:** 1917–28.
17. Counihan M.E., Shay D.K., Holman R.C., Lowther S.A., Anderson L.J. (2001) Human parainfluenza virus-associated hospitalizations among children less than five years of age in the United States. *Pediatr Infect Dis J* **20:** 646–53.
18. Fry A.M., Curns A.T., Harbour K., Hutwagner L., Holman R.C., Anderson L.J. (2006) Seasonal trends of human parainfluenza viral infections: Unites States, 1990–2004. *Clin Infect Dis* **43:** 1016–22.
19. Larurichesse H., Dedman D., Watson J.M. Zambon M.C. (1999) Epidemiological features of parainfluenza virus infections: laboratory surveillance in England and Wales, 1975–1997. *Europ J Epidemiol* **15:** 475–84.
20. Easton A.J., Eglin R.P. (1989) Epidemiology of parainfluenza virus type 3 in England and Wales over a ten-year period. *Epidemiol Infect* **102:** 531–5.

Yamagata, Japan, and epidemiologic investigation found that it was associated with HPeV3 infection. We describe this outbreak and provide expanded information about the clinical spectrum of HPeV3 infection.

Methods

Case-Patients

During June 17–August 6, 2008, an outbreak of an unknown disease was observed among adults in Yonezawa, Yamagata, Japan. A total of 22 patients who lived in the city of Yonezawa who had myalgia, muscular weakness, sore throat, and orchiodynia (among men) sought treatment at Yonezawa City Hospital. Because all had symptoms of severe myalgia, these patients were given a diagnosis of with acute myalgia syndrome of unknown cause. The patients consisted of 15 men and 7 women ages 25–66 years (mean 37 years). Because several patients had contact with other persons who had similar symptoms, the outbreak was considered to be associated with an infectious agent. Virologic and serologic analyses were carried out to find the associated agent. This study was approved by the Ethics Committee of the Yonezawa City Hospital.

Screening for Pathogens

Throat swab and stool specimens were collected from 14 patients (Table 1). Throat swab specimens were placed immediately in tubes containing 3 mL of transport medium, and stool specimens were put in a stool container and transported to the Department of Microbiology, Yamagata Prefectural Institute of Public Health, Yamagata, to undergo virus isolation and reverse transcription PCR (RT-PCR) for enteroviruses, HPeV1, and HPeV2.

Virus isolation was carried out using a described microplate method (*15*). In brief,, HEF, HEp-2, Vero E6, MDCK, RD-18S, and GMK cell lines were prepared in the wells of a 96-well microplate (Greiner Bio-One, Frickenhausen, Germany). After a medium change, throat swabs and 10% stool suspension specimens were centrifuged at 1,500 × *g* for 20 min, and 75 μL of the supernatant was added to 2 wells of each of the cell lines. The inoculated plates were centrifuged for 20 min at 450 × *g*, incubated at 33°C in a 5% CO_2 incubator, and assessed for cytopathic effect.

RNA was extracted from 200 μL of each throat swab specimen or 10% stool suspension using a High Pure Viral RNA Kit (Roche Diagnostics, Manheim, Germany) according to the manufacturer's instructions and then transcribed into complementary DNA (cDNA) as described (*16*). PCR was performed as described (*17*,*18*), except that we used a mixture of 224 and 222 primers for the first PCR and a mixture of AN89 and AN88 primers for the nested PCR to detect enteroviruses and K28, K29, and K30 primers to detect HPeV1 and HPeV2. The remainder of each specimen and the cDNA specimens were stored at −80°C.

Ultra-high Throughput Direct Sequencing Analysis

Ultra-high throughput direct sequencing analysis was carried out as described (*19*). Total DNA or RNA was prepared from the specimens of case-patient 11 by using a viral nucleic acid purification kit (Roche Diagnostics). Double-stranded cDNA (ds-cDNA) was prepared from 1 μg of total RNA using the random priming method with the SuperScript Choice System for cDNA synthesis (Invitrogen, Carlsbad, CA, USA). A mixture of DNA and ds-cDNA was purified by using a QIAquick PCR Purification kit (QIAGEN, Hilden, Germany).

An ≈300-bp length DNA library was prepared from a mixture of 2 μg of total DNA and ds-cDNA by using a genomic DNA sample prep kit (Illumina, San Diego, CA, USA), and DNA clusters were generated on a slide using a Single Read Cluster Generation kit version 4 on an Illumina cluster station (Illumina) according to the manufacturer's instructions. To obtain ≈1.0×10^7 clusters for 1 lane, the general procedure as described in the manufacturer's standard recipe was performed. All sequencing runs for 83-mers were performed with GA II using the Illumina Sequencing Kit version 5. Fluorescent images were analyzed using the Illumina SCS2.8/RTA1.8 to obtain FASTQ formatted sequence data. The obtained DNA sequence reads were investigated by using a MEGABLAST search (*20*) with an e^{-5} e-value cutoff against the nonredundant nt database nt, followed by taxonomic classification using MEGAN version 3.9.0 (*21*) with the following parameters: minimum support 1; minimum score 35.0.

RT-PCR was performed by using ≈100 ng of total RNA, the appropriate primer pair, and the PrimeScript II High Fidelity One-Step RT-PCR Kit (TaKaRa, Shiga, Japan). The following quantitative RT-PCR program was used: reverse transcription reaction 45°C for 10 min; initial denaturation 94°C for 2 min; and 3 steps of amplification (× 35 cycles) at 98°C for 10 s, 55°C for 15 s, and 68°C for 1 min. PCR products were resolved and purified by agarose gel electrophoresis and then sequenced by Sanger sequencing by using a BigDye Terminator v3.1 Cycle Sequencing Kit (Applied Biosystems, Foster City, CA, USA).

Repeat of Virus Isolation and Molecular Detection for HPeV3

After HPeV3 was detected in the specimens from case-patient 11 by ultra-high throughput direct sequencing analysis, to investigate whether HPeV3 was associated with the myalgia epidemic, we repeated the virus isolation focusing on HPeV3, using GMK, Vero, and LLC-MK2 cell lines using the 28 stocked throat swab and stool samples

shown in Table 1. We used 2 LLC-MK2 cell lines, one provided by the National Institute of Infectious Diseases Japan and the other by the Niigata Prefectural Institute of Public Health and Environmental Sciences. We also attempted to specifically amplify the HPeV3 genome via RT-PCR using frozen cDNA and our original primers (Parecho3-VP1F1Y and Parecho3-VP1R1Y for the first PCR and Parecho3-VP1F2Y and Parecho3-VP1R2Y for the nested PCR [Table 2, Appendix, wwwnc.cdc.gov/EID/article/18/11/11-1570-T2.htm]), using the same conditions as in the preliminary screening procedure. When the RT-PCR result was positive, PCR products were purified and sequenced on a Sanger sequencer using a BigDye Terminator v3.1 Cycle Sequencing Kit (Applied Biosystems) and the primers listed in Table 2, Appendix. We also attempted to amplify the HPeV3 genome using RT-PCR from all serum specimens that were initially collected for serologic analysis.

Serologic Study

To further evaluate the role of HPeV3 in this outbreak of myalgia, we measured the neutralizing antibody response against HPeV3 in 1–5 serum samples from 20 of the patients (Table 1). To observe seroconversion and changes in antibody titers, we measured neutralization antibodies using a microneutralization test on a 96-well microplate. Sample serum samples were inactivated at 56°C for 30 min and then diluted from 1:8 to 1:4,096 by serial 2-fold dilution. One HPeV3 isolate in this outbreak in Yamagata (1356-Yamagata-2008) was used as a challenge virus antigen. We mixed and incubated (37°C, 60 min) 60 μL of each diluted serum sample with 60 μL of virus fluid containing ≈10^2 50% tissue culture infectious dose. We prepared confluent monolayers of the LLC-MK2 cell line provided by the Niigata Prefectural Institute of Public Health and Environmental Sciences, washed the cells with phosphate-buffered saline without calcium or magnesium, added 50 μL of maintenance media, and injected 50 μL of each incubated virus–serum mixture into each of 2 cultures. The plates were then incubated in a 5% CO_2 incubator at 33°C for cytopathic effect observation. The reciprocal value of the highest dilution of serum neutralizing the virus compared to the control was taken to be the titer. Seropositivity was defined as titer ≥8. Virus infection was

Table 2. Primers used to detect and sequence analysis for human parechovirus 3 among patients with epidemic myalgia, Yonezawa, Yamagata, Japan, June–August 2008

Primer	Nucleotide sequence, 5′ → 3′	Nucleotide position*
Parecho3-F2K	AACAAGTGACACTATGGATCTGATC	576–601
Parecho3-F3K	CAAAGTAGCAGATGATGCTTCCAA	824–849
Parecho3-F4K	CAAGCCAAATATTTTGCTGCAGTAA	1165–1190
Parecho3-F5K	TGCATTGGTGGTTTATGAGCCTAA	1244–1268
Parecho3-F21K	TCAGACAACACCACACCTTCAAG	1822–1844
Parecho3-VP1F1Y	GGGCCTTTGGGTAATGAGAAA	2452–2472
Parecho3-VP1F2Y	TGACAACATATTTGGTAGAGCTTGGT	2538–2563
Parecho3-F6K	AGGAGATAATGTATATCAATTGGAT	3095–3120
Parecho3-F7K	TGACGGCTGGTTTAATGTCAACTAT	3368–3392
Parecho3-F8K	CTGAATCAATGTCCAACACAGACGA	3737–3761
Parecho3-F9K	TGGACTATGCCTCTGATATTATTGT	3994–4019
Parecho3-F10K	AATAATGGCCATTTGCTTTAGGAGT	4098–4122
Parecho3-F11K	CTTGTAAATTAAATGGTGTGTACAC	4304–4328
Parecho3-F12K	ACTAGGAAGGAGAAAGATATTGAAA	4402–4426
Parecho3-F13K	CAGCCAAAGCATATAGTAGGGCTG	4609–4633
Parecho3-F14K	TTGAACAAATGGAAGCCTTCATTGA	4916–4940
Parecho3-F15K	GTTGTAGACTGGTTCAGTAGTAAG	5011–5034
Parecho3-F16K	AAAGGAACTTTCCCAGTCACGCAGA	5201–5225
Parecho3-F17K	CAGAGAGTATGTTGATTTGGATGAC	5553–5576
Parecho3-F18K	GTGGCTATTCCTTTCAATTTTCTT	5778–5802
Parecho3-F19K	GGCCCAGCAGTTTTAAGCAAATCAG	5863–5947
Parecho3-F20K	TTGTCATGATTCACCTGATCTTGTC	6608–6633
Parecho3-R13K	AGTTTGTGGTATTTACAGTGGTTGT	912–938
Parecho3-R11K	TTTTAACGTAGTTTGTGTCTGCA	1380–1402
Parecho3-R15	CATGTATAGAATATGAATGTTTATT	2673–2697
Parecho3-VP1R2Y	ACCCCTGCTCTGCCATGTATA	2693–2710
Parecho3-VP1R1Y	TCCCGTGCATCATTGGTCTA	2883–2902
Parecho3-R10K	TGACAGATGATTCAAGATACTTCAC	3238–3253
Parecho3-R9K	AGTGGTACACTTCTGCACAAGTAAG	3468–3492
Parecho3-R8K	ATCCACCAATCAATATGTCTGAATG	3859–3884
Parecho3-R7K	TGGATAGTGTGTGTGTTAGGAAAGA	4264–4288
Parecho3-R5K	CCACTTTAGAAATAAGCAGACCACC	5701–5725
Parecho3-R4K	CCATTTTGACTTCCACTGCTCCA	5901–5923
Parecho3-R3K	CCTAAATTTGGACTTGACACAGG	5993–6015
HPeV3whole-RT-RK	TTTTGGTATGTCCAATATTCCAAATTAGTG	7296–7321

*Relative to human parechovirus 3 strain A308/99 (GenBank accession no. AB084913).

considered confirmed if seroconversion from negative to positive could be documented. Alternatively, if all serum samples were positive, a 4-fold increase in antibody titer was considered serologic evidence of infection with HPeV3.

Results

Case-Patients

The 22 case-patients in this outbreak had similar symptoms (Table 1); all had severe myalgia involving mainly the proximal muscles of the upper and lower extremities. The next most common symptom was muscular weakness in the arms and legs (21, 95.5%), followed by fever (19, 86.4%), pharyngitis (15, 68.2%), orchiodynia (4, 18.2%), and seizures (1, 4.5%). Symptoms worsened rapidly within 1–2 days after onset. Eight patients were hospitalized on a visit to Yonezawa City Hospital and remained hospitalized for 5 (4 patients), 6 (1 patient), 8 (2 patients), or 10 days (1 patient); mean hospitalization was 6.5 days. Case-patient 14 had seizures and subsequent disturbance of consciousness. For all patients, muscular weakness improved as muscle pain decreased.

Laboratory Findings

Creatinine phosphokinase (CPK), C-reactive protein, and myoglobin levels were higher than reference ranges in 12, 19, and 16 patients, respectively (Table 1). Elevated CPK levels returned to normal within several days. An examination of cerebrospinal fluid showed no sign of inflammation.

Magnetic resonance imaging (MRI) of the muscles of case-patients 4, 13, and 15 showed increased signal intensity on T2-weighted images. We suspected that case-patient 14 had encephalitis on the basis of clinical symptom, but results of MRI of the brain and cerebrospinal fluid examination did not support this diagnosis. Clinical symptoms and laboratory findings for all patients were consistent with inflammatory myositis.

Detection of Potential Pathogens

No viruses were detected by screening steps at the Yamagata Prefectural Institute of Public Health using virus isolation and RT-PCR targeting enteroviruses, HPeV1, and HPeV2. Thus, we investigated possible uncharacterized pathogens by using direct DNA sequencing. To determine potential pathogens for the patients, we performed direct sequencing of a mixture of purified DNA and ds-cDNA from the total RNA extracted from either the throat swab or stool specimens of case-patient 11. No other possible viral sequences were detected by the high-throughput sequencing for case-patient 11.

Next-generation DNA sequencer GA II produced $\approx 1.5 \times 10^7$ 83-mer short reads from the mixed DNA library. To exclude the human-derived read sequences, all obtained reads were initially aligned to a reference sequence of human genomic DNA, followed by quality trimming to remove low-quality reads and exclude reads with similarities to ambiguous human sequences. All remaining possible pathogen reads were further analyzed using a MegaBLAST search against nonredundant databases.

One type of HPeV was found in the analyzed specimens. Three HPeV reads were identified from the throat swab specimen and 1,505 HPeV reads from the stool specimen of case-patient 11. To further characterize the type of HPeVs detected, de novo assembly was performed by using Euler-SR version 1.0 (*22*); the resulting partial contigs showed higher similarity to HPeV3 than to other HPeVs.

To determine the whole HPeV sequence for the isolates we obtained, RT-PCR was performed (Figure 1), and the products were sequenced. The whole coding nucleotide sequence of the polyprotein in the HPeV detected in the stool sample from case-patient 11 was aligned against all available HPeV complete genomes, including HPeV1–8. A phylogenetic tree was generated for the VP1 region (Figure 2), and the HPeV in the stool specimen of case-patient 11 was identified as HPeV3. All detected HPeV3 VP1 sequences among the 2008 myalgia cases were identical (Table 1), except that we found a single nucleotide substitution in sequences from the serum samples from case-patients 4 and 22.

Repeat of Virus Isolation and Molecular Detection Targeting HPeV3

We passaged isolates 6 times using GMK and LLC-MK2 cell lines, but all strains except 1 (isolated after 5 passages) were recovered within 3–4 passages. We could not isolate HPeV3 using the LLC-MK2 cell line provided by the National Institute of Infectious Diseases Japan, but we were successful when using LLC-MK2 cell line from the Niigata Prefectural Institute of Public Health and Environmental Sciences. In total, we isolated HPeV3 strains from either the throat swab or stool specimen of 7/14 patients analyzed (Table 1).

RT-PCR was successful in detecting the HPeV3 genome in the throat swabs or stool specimens from 9/14 patients (Table 1). We also detected the HPeV3 genome in 3 serum specimens collected within 3 days after the onset of illness (Table 1). Sequence data were registered under GenBank accession nos. AB668029–AB668045.

Serologic Study

Of 20 analyzed patients, seroconversion was observed in 6 patients. A 4-fold increase in neutralization antibodies against HPeV3 was confirmed in 5 patients (Table 1).

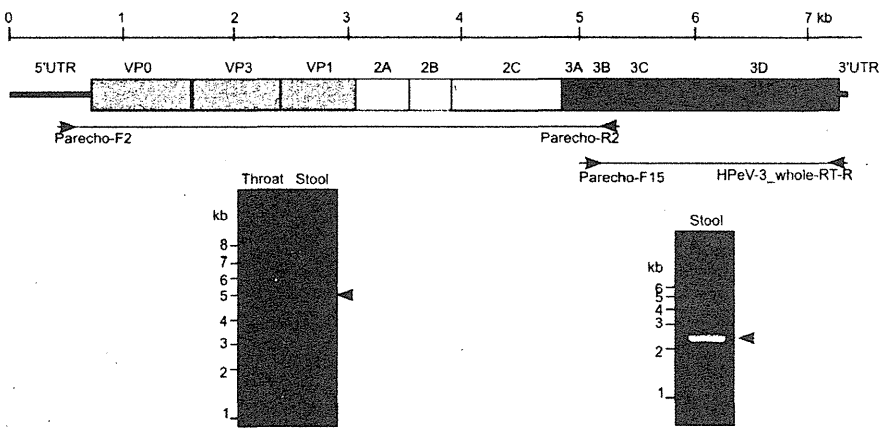

Figure 1. Schematic representation of the human parechovirus 3 (HPeV3) genome sequence and coding polyprotein. Reverse transcription PCR results are shown below the sequence. VP, viral protein; UTR, untranslated region.

Discussion

By conducting virus isolation, RT-PCR, and serologic examination, we confirmed an outbreak of epidemic myalgia among adults in Yonezawa, Yamagata, Japan, during June–August 2008 was associated with HPeV3 infection. Although we did not detect any virus in our first screening, direct sequencing analysis suggested that these patients were infected with HPeV3. We next tried to detect this virus specifically and isolated HPeV3 strains from the throat swabs or stool specimens of 7 patients; detected the virus genome in the throat swabs or stool or serum specimens of 11 patients; and observed seroconversion or 4-fold increases in antibodies against HPeV3 in 11 patients. Altogether, we confirmed HPeV3 infection in 14 of the 22 patients in this outbreak. All patients, except 1 who experienced complications related to epilepsy, recovered completely within 1 week after the onset of illness through treatment with antiinflammatory drugs only.

Enteroviruses have been implicated in the pathogenesis of human neuromuscular diseases because of their association with certain acute and chronic acquired myopathies and paralytic motor neuron syndromes (*23*). Epidemic pleurodynia (Bornholm disease), an acute febrile illness with myalgia caused by picornaviruses such as group B coxsackieviruses, is perhaps best known (*24–26*). However, in this outbreak, none of the patients showed the chest and abdominal pain typical of pleurodynia; they instead showed muscular weakness, which is not generally observed in epidemic pleurodynia (*23,25*). Conversely, it has been reported that patients with acute enterovirus myositis experience fever, chills, myalgia, and generalized weakness and that thigh muscle or generalized muscle involvement may occur (*25,26*). Among these patients, laboratory studies may demonstrate myoglobinemia, myoglobinuria, and an elevated levels of muscle enzymes such as CPK (*25,26*). The HPeV3 outbreak in Yonezawa resembles these descriptions of acute myositis outbreaks; patients commonly had fever, myalgia, and muscle weakness mainly in the arms and legs, and laboratory findings and MRI studies suggested the presence acute inflammation around the peripheral muscles. Thus, we concluded that the disease in this outbreak was an acute inflammatory muscle disease associated with HPeV3 infection in adults.

In enterovirus viremia, viruses enter through the oral or respiratory route, replicate in the pharynx and alimentary tract, spread to multiple organs such as the central nervous system, heart, and skin, and then diminish and disappear after neutralizing serum antibodies are produced (*24*). HPeV3 has been reported to cause severe systemic diseases, especially in neonates and infants (*1,7,11,13*). HPeV3 has been isolated using the Vero cell line or detected by real-time PCR in not only nasopharyngeal swabs but also in the lungs, colons, and spleens of dead infants (*27*).

In this study, we showed HPeV3 viremia in 3 patients without neutralizing antibodies within a few days after the onset of illness. Thus, we conclude that HPeV3 viremia affects many organs, including the peripheral muscles as well as the organs normally targeted by enteroviruses. Several male patients in the Yonezawa outbreak also had orchitis, which is described as a symptom of epidemic pleurodynia (*24*) but may also be associated with systemic infection, although we have no evidence to support this hypothesis.

HPeV often grows poorly in culture, and typing reagents are not widely available for newly discovered types (HPeV3–14) (*1,28*). In particular, HPeV3 is difficult to culture in standard diagnostic cell lines, and its isolation is largely determined by the cell lines used (*14*). So far, Vero, LLC-MK2, Caco2, and BSC-1 cell lines have been used (*3,7,8,10,14,27*). In the first screening in our study, we could not isolate HPeV3 using 6 cell lines that we use routinely (*15*). However, we succeeded in whole-sequence analysis using a stool specimen from case-patient 11, which

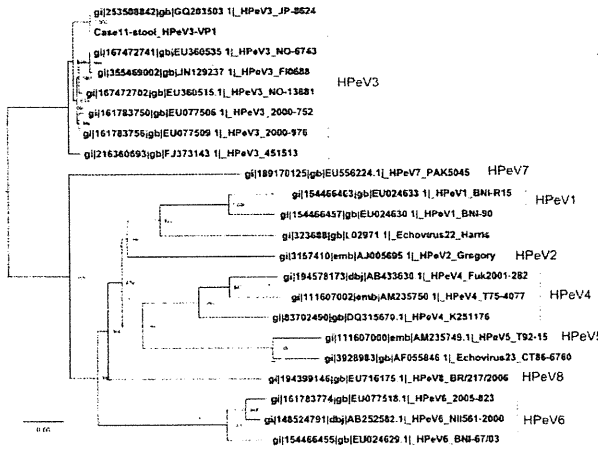

Figure 2. Phylogenetic tree of the viral protein 1 region sequence in the available human parechovirus (HPeV) genomes, including HPeV1–8. The tree was constructed by the neighbor-joining method with 1,000× bootstrapping. Scale bar indicates nucleotide substitutions per site.

suggests the failure to isolate HPeV3 was not a result of low viral load in the specimens from the patients with epidemic myalgia. In our second attempt at isolation using several monkey kidney cell lines, such as GMK and LLC-MK2, we were able to isolate HPeV3 after only several passages. Although 2 LLC-MK2 cell lines were used for HPeV3 isolation, the susceptibility of the lines to HPeV3 infection differed, further demonstrating the difficulties in culturing HPeV3. Because we analyzed a range of respiratory viruses, which are isolated from nasopharyngeal specimens, we routinely culture specimen-inoculated plates at 33°C; however, to isolate HPeV3, plates should be cultured at 37°C.

Although we used a new direct-sequence analysis method and a slightly older RT-PCR method to amplify the HPeV3 genome in this study, new laboratory diagnostic procedures for HPeVs have been developed during the past few years. HPeV RT-PCRs now exist to detect all known HPeV types with great sensitivity (*29*), and HPeV3 and all the other HPeVs can be typed by nested or semi-nested PCR coupled with sequencing of the VP1 gene (*30*).

Our finding of HPeV3 infection in adults conflicts with most of the literature, which suggests that HPeV3 infections occur in early infancy (*1,3,7,10,11,13*). Harvala et al. observed that HPeV3 infections were seen exclusively in children <3 months of age (*1,11,13*). Watanabe et al. reported that HPeV3 was isolated from a 35-year-old woman with influenza-like illness, while 12/16 HPeV3-isolated cases were from patients <3 years of age (*14*). Our findings show that epidemic myalgia associated with HPeV3 infection might occur among adults, particular among those ≈30–40 years of age.

It remains unclear why these HPeV3 infections occurred among adults in 2008. HPeV3 infections occur in the spring and summer seasons, whereas HPeV1 infections are observed in small numbers throughout the year but predominantly during the fall and winter (*9,10,12,31*). National surveillance data for infectious diseases in Japan show HPeV3 yearly detection numbers was 1, 2, 52, 1, and 81 cases each year for 2004–2008; 117 cases (85.4%) were detected during June–September (*32*). The higher number of cases in 2008, coupled with a reported epidemic of HPeV3 among children, most <3 months of age, in Hiroshima Prefecture, Japan (*33*), indicates a possible summer outbreak of HPeV3 in 2008 in Japan. We postulate that an outbreak of HPeV3 among children was a necessary background condition for the outbreak of epidemic myalgia among adults in 2008.

In conclusion, we document detection of HPeV3 infection among adult patients with epidemic myalgia in Yamagata, Japan, during 2008. Clinical consideration should be given to HPeV3 not only in young children but also in adults when an HPeV3 outbreak occurs in the community. Continued research on adults with HPeV3 infection is needed to further understand the etiology and epidemiology of HPeV3.

Acknowledgments

We thank the medical staff and people of the Yamagata Prefecture for their collaboration in specimen collection for the surveillance of viral infectious diseases. We also thank M. Kon and T. Tamura and the Niigata Prefectural Institute of Public Health and Environmental Sciences for providing us with LLC-MK2 cell line.

This work was supported by a grant-in-aid from the Japan Society for the Promotion of Science and for Research on Emerging and Re-emerging Infectious Diseases of the Ministry of Health, Labour and Welfare, Japan.

Dr Mizuta is the vice-director of Yamagata Prefectural Institute of Public Health, Yamagata, Japan. His research focuses on epidemiology and etiology of respiratory viruses.

References

1. Harvala H, Simmonds P. Human parechoviruses: biology, epidemiology and clinical significance. J Clin Virol. 2009;45:1–9. http://dx.doi.org/10.1016/j.jcv.2009.03.009
2. Stanway G, Joki- Korpela P, Hyypiä T. Human parechovirus – biology and clinical significance. Rev Med Virol. 2000;10:57–69. http://dx.doi.org/10.1002/(SICI)1099-1654(200001/02)10:1<57::AID-RMV266>3.0.CO;2-H
3. Ito M, Yamashita T, Tsuzuki H, Takeda N, Sakae K. Isolation and identification of a novel human parechovirus. J Gen Virol. 2004;85:391–8. http://dx.doi.org/10.1099/vir.0.19456-0
4. Picornavirus homepage [cited 2012 Apr 16]. http://www.picornaviridae.com/parechovirus/hpev/hpev_seqs.htm

5. Knowles NJ, Hovi T, King AMQ, Stanway G. Overview of taxonomy. In: Ehrenfeld E, Domingo E, Roos RP, editors. The Picornaviruses. Washington (DC): ASM Press; 2010. p. 26.
6. Khetsuriani N, LaMonte A, Oberste MS, Pallansch M. Neonatal enterovirus infections reported to the National Enterovirus Surveillance System, 1983–2003. Pediatr Infect Dis J. 2006;25:889–93. http://dx.doi.org/10.1097/01.inf.0000237798.07462.32
7. Boivin G, Abed Y, Boucher FD. Human parechovirus 3 and neonatal infections. Emerg Infect Dis. 2005;11:103–7. http://dx.doi.org/10.3201/eid1101.040606
8. Abed Y, Boivin G. Human parechovirus infections in Canada. Emerg Infect Dis. 2006;12:969–75. http://dx.doi.org/10.3201/eid1206.051675
9. Benschop KSM, Schinkel J, Minnaar RP, Pajkrt D, Spanjerberg L, Kraakman HC, et al. Human parechovirus infections in Dutch children and the association between serotype and disease severity. Clin Infect Dis. 2006;42:204–10. http://dx.doi.org/10.1086/498905
10. van der Sanden S, de Bruin E, Vennema H, Swanink C, Koopmans M, van der Avoort H. Prevalence of human parechovirus in the Netherlands in 2000 to 2007. J Clin Microbiol. 2008;46:2884–9. http://dx.doi.org/10.1128/JCM.00168-08
11. Harvala H, Robertson I, Chieochansin T, McWilliam Leitch EC, Templeton K, Simmonds P. Specific association of human parechovirus type 3 with sepsis and fever in young infants, as identified by direct typing of cerebrospinal fluid samples. J Infect Dis. 2009;199:1753–60. http://dx.doi.org/10.1086/599094
12. Selvarangan R, Nzabi M, Selvaraju SB, Ketter P, Carpenter C, Harrison CJ. Human parechovirus 3 causing sepsis-like illness in children from Midwestern United States. Pediatr Infect Dis J. 2011;30:238–42. http://dx.doi.org/10.1097/INF.0b013e3181fbefc8
13. Harvala H, McLeish N, Kondracka J, McIntyre CL, McWilliam Leitch EC, Templeton K, et al. Comparison of human parechovirus and enterovirus detection frequencies in cerebrospinal fluid samples collected over a 5-year period in Edinburgh: HPeV type 3 identified as the most common picornavirus type. J Med Virol. 2011;83:889–96. http://dx.doi.org/10.1002/jmv.22023
14. Watanabe K, Oie M, Higuchi M, Nishikawa M, Fujii M. Isolation and characterization of novel human parechovirus from clinical samples. Emerg Infect Dis. 2007;13:889–95. http://dx.doi.org/10.3201/eid1306.060896
15. Mizuta K, Abiko C, Aoki Y, Suto A, Hoshina H, Itagaki T, et al. Analysis of monthly isolation of respiratory viruses from children by cell culture using a microplate method: a two-year study from 2004 to 2005 in Yamagata, Japan. Jpn J Infect Dis. 2008;61:196–201.
16. Murata T, Katsushima N, Mizuta K, Muraki Y, Hongo S, Matsuzaki Y. Prolonged norovirus shedding in infants ≈6 months of age with gastroenteritis. Pediatr Infect Dis J. 2007;26:46–9. http://dx.doi.org/10.1097/01.inf.0000247102.04997.e0
17. Nix WA, Oberste MS, Pallansch MA. Sensitive, seminested PCR amplification of VP1 sequences for direct identification of all enterovirus serotypes from original clinical specimens. J Clin Microbiol. 2006;44:2698–704. http://dx.doi.org/10.1128/JCM.00542-06
18. Oberste MS, Maher K, Pallansch MA. Specific detection of echoviruses 22 and 23 in cell culture supernatants by RT-PCR. J Med Virol. 1999;58:178–81. http://dx.doi.org/10.1002/(SICI)1096-9071(199906)58:2<178::AID-JMV13>3.0.CO;2-Q
19. Kuroda M, Katano H, Nakajima N, Tobiume M, Ainai A, Sekizuka T, et al. Characterization of quasispecies of pandemic 2009 influenza A virus (A/H1N1/2009) by *de novo* sequencing using a next-generation DNA sequencer. PLoS ONE. 2010;5:e10256. http://dx.doi.org/10.1371/journal.pone.0010256
20. Morgulis A, Coulouris G, Raytselis Y, Madden TL, Agarwala R, Schäffer AA. Database indexing for production MegaBLAST searches. Bioinformatics. 2008;15:1757-1764.
21. Huson DH, Mitra S, Ruscheweyh HJ, Weber N, Schuster SC. Integrative analysis of environmental sequences using MEGAN4. Genome Res. 2011;21:1552–60. http://dx.doi.org/10.1101/gr.120618.111
22. Chaisson MJ, Brinza D, Pevzner PA. De novo fragment assembly with short mate-paired reads: Does the read length matter? Genome Res. 2009;19:336-46.
23. Dalakas MC. Enteroviruses and human neuromuscular diseases. In: Rotbart HA, editor. Human enterovirus infections. Washington (DC): ASM Press; 1995. p. 387–98.
24. Cherry JD, Krogstad P. Enteroviruses and parechoviruses. In: Feigin RD, Cherry JD, Demmler-Harrison GJ, Kaplan SL, editors. Textbook of pediatric infectious diseases. Philadelphia: Saunders Elsevier; 2009. p. 2110–70.
25. Pallansch M, Roos R. Enteroviruses: polioviruses, coxsackieviruses, echoviruses, and newer enteroviruses. In: Knipe DM, Howley PM, editors. Fields virology, 5th ed. Philadelphia: Lippincott Williams & Wilkins; 2007. p. 839–93.
26. Modin JF. Enteroviruses. In: Gershon AA, Hotez PJ, Katz SL, eds. Infectious diseases in children. Philadelphia: Mosby; 2004. p. 117–42.
27. Sedmak G, Nix WA, Jentzen J, Haupt TE, Davis JP, Bhattacharyya S, et al. Infant deaths associated with human parechovirus infection in Wisconsin. Clin Infect Dis. 2010;50:357–61. http://dx.doi.org/10.1086/649863
28. Benschop K, Minnaar R, Koen G, van Eijk H, Dijkman K, Westerhuis B, et al. Detection of human enterovirus and human parechovirus (HPeV) genotypes from clinical stool samples: polymerase chain reaction and direct molecular typing, culture characteristics, and serotyping. Diagn Microbiol Infect Dis. 2010;68:166–73. http://dx.doi.org/10.1016/j.diagmicrobio.2010.05.016
29. Nix WA, Maher K, Johansson ES, Niklasson B, Lindberg AM, Pallansch MA, et al. Detection of all known parechoviruses by real time-PCR. J Clin Microbiol. 2008;46:2519–24. http://dx.doi.org/10.1128/JCM.00277-08
30. Nix WA, Maher K, Pallansch MA, Oberste MS. Parechovirus typing in clinical specimens by nested or semi-nested PCR coupled with sequencing. J Clin Virol. 2010;48:202–7. http://dx.doi.org/10.1016/j.jcv.2010.04.007
31. Ito M, Yamashita T, Tsuzuki H, Kabashima Y, Hasegawa A, Nagaya S, et al. Detection of human parechoviruses from clinical stool samples in Aichi, Japan. J Clin Microbiol. 2010;48:2683–8. http://dx.doi.org/10.1128/JCM.00086-10
32. Infectious Diseases Surveillance Center, National Institute of Infectious Diseases Japan. Infectious Agents Surveillance Report [cited 2011 Aug 2]. http://idsc.nih.go.jp/iasr/virus/pvirus-j.html
33. Yamamoto M, Abe K, Kuniyori K, Kunii E, Ito F, Kasama Y, et al. Epidemic of human parechovirus type 3 in Hiroshima city, Japan, in 2008. Jpn J Infect Dis. 2009;62:244–5.

Address for correspondence: Katsumi Mizuta, Department of Microbiology, Yamagata Prefectural Institute of Public Health, Tokamachi 1-6-6, Yamagata 990-0031, Japan; email: mizutak@pref.yamagata.jp

Epidemic Myalgia in Adults Associated with Human Parechovirus Type 3 Infection, Yamagata, Japan, 2008

Katsumi Mizuta, Makoto Kuroda, Masayuki Kurimura, Yoshikazu Yahata, Tsuyoshi Sekizuka, Yoko Aoki, Tatsuya Ikeda, Chieko Abiko, Masahiro Noda, Hirokazu Kimura, Tetsuya Mizutani,[1] Takeo Kato, Toru Kawanami, and Tadayuki Ahiko

Human parechovirus has rarely been shown to cause clinical disease in adults. During June–August 2008, a total of 22 adults sought treatment at Yonezawa City Hospital in Yamagata, Japan, for muscle pain and weakness of all limbs; most also had fever and sore throat. All patients received a clinical diagnosis of epidemic myalgia; clinical laboratory findings suggested an acute inflammatory process. Laboratory confirmation of infection with human parechovirus type 3 (HPeV3) was made for 14 patients; we isolated HPeV3 from 7 patients, detected HPeV3 genome in 11, and observed serologic confirmation of infection in 11. Although HPeV3 is typically associated with disease in young children, our results suggest that this outbreak of myalgia among adults was associated with HPeV3 infection. Clinical consideration should be given to HPeV3 not only in young children but also in adults when an outbreak occurs in the community.

Human parechovirus (HPeV) is a positive-sense, single-stranded RNA virus belonging to the family *Picornaviridae* and the genus *Parechovirus* (*1*,*2*). HPeV type 1 (HPeV1) and HPeV2 were discovered in the United States in children with diarrhea in 1956; initially designated echovirus types 22 and 23, respectively, these viruses were recently reclassified and renamed (*1*,*2*). In 1999, HPeV3 was identified from a 1-year-old child with transient paralysis, fever, and diarrhea in Japan (*3*). Complete genome sequences are available for HPeV1–8, and viral protein (VP) 1 coding region sequences have recently been reported for HPeV9–16 (*1*,*4*).

HPeV1 and HPeV2 mainly cause mild gastrointestinal or respiratory illness, but more serious diseases have been occasionally reported, including myocarditis, encephalitis, pneumonia, meningitis, flaccid paralysis, Reye syndrome, and fatal neonatal infection (*2*,*5*,*6*). HPeV3 also causes not only mild gastrointestinal and respiratory tract illness but also severe illness in young children, including sepsis and conditions involving the central nervous system (*1*,*5*,*7*–*13*).

Although the seroprevalence of the recently discovered HPeV4–8 are unknown, HPeV1–3 infections usually occur in early infancy (*1*,*3*). Because all children have antibodies against HPeV1 after 1 year of age, HPeV1 seroconversion during the early months of life has been clearly established (*2*). HPeV3 is reported to infect younger children more often than HPeV1; HPeV3 infections occur most commonly among infants <3 months of age (*1*,*10*,*11*). In contrast, reports in the literature that describe HPeV3 infection in persons >10 years of age are rare (*1*,*14*).

An unusual outbreak of epidemic myalgia among adults occurred during June–August 2008 in Yonezawa,

Author affiliations: Yamagata Prefectural Institute of Public Health, Yamagata, Japan (K. Mizuta, Y. Aoki, T. Ikeda, C. Abiko, T. Ahiko); National Institute of Infectious Diseases, Tokyo, Japan (M. Kuroda, T. Sekizuka, M. Noda, H. Kimura, T. Mizutani); Yonezawa City Hospital, Yamagata (M. Kurimura, Y. Yahata); and Yamagata University Faculty of Medicine, Yamagata (T. Kato, T. Kawanami)

DOI: http://dx.doi.org/10.3201/eid1811.111570

[1]Current affiliation: Tokyo University of Agriculture and Technology Research and Education Center for Prevention of Global Infectious Diseases of Animals, Tokyo, Japan.

VIROLOGY

Interferon-Induced SCYL2 Limits Release of HIV-1 by Triggering PP2A-Mediated Dephosphorylation of the Viral Protein Vpu

Kei Miyakawa,[1,2] Tatsuya Sawasaki,[3] Satoko Matsunaga,[1] Andrey Tokarev,[4] Gary Quinn,[1] Hirokazu Kimura,[5] Masako Nomaguchi,[6] Akio Adachi,[6] Naoki Yamamoto,[7] John Guatelli,[4,8] Akihide Ryo[1]*

Human cells respond to infection by retroviruses through the actions of proteins that inhibit the spread of viruses to other cells. One example is bone marrow stromal cell antigen 2 (BST2; also known as tetherin), which is an interferon (IFN)–inducible protein that restricts the release of progeny virions from infected cells. The HIV-1 accessory protein Vpu (viral protein U) causes degradation of BST2, and phosphorylation of Vpu at residues Ser^{52} and Ser^{56} is required for this function. We report that the host protein SCY1-like protein 2 (SCYL2) mediates the dephosphorylation of Vpu, antagonizing Vpu function and facilitating BST2-dependent restriction of HIV-1 release. SCYL2 reduced the number of virus particles released from cells infected with wild-type HIV-1, but not a strain lacking *vpu*, in a BST2-dependent manner. SCYL2 stimulated the dephosphorylation of Vpu on Ser^{52} and Ser^{56} by recruiting protein phosphatase 2A (PP2A) to Vpu. Conversely, depletion of SCYL2 resulted in enhanced phosphorylation of Vpu and increased viral particle release. Moreover, SCYL2 was produced in response to type I IFN and contributed to IFN-mediated viral restriction. Together, these results suggest that SCYL2 serves as a regulatory factor for Vpu, reducing the extent of Vpu phosphorylation and consequently enhancing BST2-mediated viral restriction.

INTRODUCTION

Accumulating evidence indicates that the HIV-1 accessory proteins antagonize host defenses to support efficient viral replication (*1*–*5*). Viral protein U (Vpu) is an 81–amino acid residue accessory protein that is encoded by HIV-1, simian immunodeficiency virus isolated from chimpanzees (SIV_{CPZ}), and some SIVs isolated from Old World monkeys (the SIV_{GSN} lineage). Vpu is translated from a bicistronic mRNA that also encodes the viral envelope glycoprotein (Env) (*6*–*8*). Although Vpu is not absolutely required for HIV-1 replication (*6*), studies with molecular clones of virus lacking *vpu* have demonstrated that the Vpu protein substantially enhances the production of infectious virus through at least two distinct mechanisms: the proteasomal degradation of CD4 (*9*) and the functional inactivation of the interferon (IFN)–inducible restriction factor bone marrow stromal cell antigen 2 (BST2; also known as tetherin) (*10*, *11*).

Cell-surface CD4 acts as an entry receptor for HIV-1, but it also inhibits viral release and virion infectivity (*12*, *13*). CD4 binds to the Env precursor protein gp160 in the endoplasmic reticulum (ER) and inhibits its processing to gp120 and gp41. Vpu physically interacts with CD4 in the ER and facilitates its degradation, enabling Env processing and the efficient production of infectious virions (*14*). The restriction factor BST2 inhibits viral particle release, but similar to the effects of CD4, this inhibition is functionally counteracted by Vpu (*10*, *11*). Vpu reduces the cell-surface abundance of BST2 through transmembrane interactions (*11*, *15*–*21*), and it directs the degradation of BST2, primarily in lysosomes (*15*–*17*, *22*–*25*). In the absence of Vpu, BST2 cross-links nascent virions to the plasma membrane of infected cells and substantially inhibits the release of viral particles (*26*–*28*).

Previous reports indicated that Vpu is phosphorylated, presumably by casein kinase II (CKII), on two phospho-acceptor sites (Ser^{52} and Ser^{56}) in its cytoplasmic domain (*29*, *30*). Phosphorylation of both residues is required for efficient Vpu-mediated removal of BST2 from the cell surface as well as for the degradation of CD4 (*15*, *23*, *24*, *31*, *32*). The amino acid sequence of the region of Vpu ($DpS^{52}GxxpS^{56}$) that contains both phosphorylated serines (pS) residues is recognized by an F-box–containing ubiquitin ligase subunit, β transducin repeat–containing protein (β-TrCP). Vpu thus recruits the multisubunit SCF (Skp1-Cullin-F-box)–β-TrCP E3 ubiquitin ligase complex, which leads to the ubiquitination and degradation of BST2 and CD4 (*15*, *23*, *24*, *33*). Indeed, an HIV-1 clone carrying a mutation in the β-TrCP–binding motif of Vpu fails to reduce BST2 abundance in infected T cells (*15*, *34*). Although the phosphorylation of Vpu on Ser^{52} and Ser^{56} is a crucial step in the Vpu-dependent inhibition of BST2, how this process is further regulated is not well understood.

The type I IFN system, which includes IFN-α and IFN-β, is an innate immune response to viral infection and creates an antiviral state in cells that provides an important first line of defense against viral infection (*35*). Type I IFN is widely believed to have an inhibitory effect on HIV-1 replication (*36*). The biological response to IFN is mediated by its binding to the IFN receptors and the activation of the Janus-activated kinase (JAK)–signal transducer and activator of transcription (STAT) pathway, which leads to the expression of several hundred IFN-stimulated genes (ISGs) (*37*). Although BST2 has been described as an ISG (*38*), Vpu targets

[1]Department of Microbiology, Yokohama City University School of Medicine, Kanagawa 236-0004, Japan. [2]Japanese Foundation for AIDS Prevention, Tokyo 101-0061, Japan. [3]Cell-Free Science and Technology Research Center, Ehime University, Ehime 790-8577, Japan. [4]Department of Medicine, University of California, La Jolla, CA 92093, USA. [5]Infectious Disease Surveillance Center, National Institute of Infectious Diseases, Tokyo 208-0011, Japan. [6]Department of Microbiology, Institute of Health Biosciences, The University of Tokushima Graduate School, Tokushima 770-8503, Japan. [7]Department of Microbiology, National University of Singapore, Singapore 117597, Singapore. [8]San Diego Veterans Affairs Healthcare System, San Diego, CA 92161, USA.
*To whom correspondence should be addressed. E-mail: aryo@yokohama-cu.ac.jp

IFN-induced BST2 for removal from the cell surface, which is the apparent site of action of BST2 as a restriction factor. This suggests that Vpu plays a major role in conferring resistance on the innate immune response. However, treatment of HIV-1–infected cells with type I IFN can suppress viral particle release even in the presence of Vpu (*39–41*). This finding prompted us to hypothesize that the function of Vpu could be modulated by other host factors that would likely be induced by type I IFN; however, no such factor has yet been identified. To identify host factors that regulate Vpu activity, we used an in vitro, high-throughput protein-protein interaction assay with full-length HIV-1 Vpu and host kinase–related proteins synthesized in the wheat cell-free protein production system. Here, we report that SCY1-like protein 2 (SCYL2) is a functional interactor of Vpu and that it inhibits Vpu function by promoting the dephosphorylation of Vpu by the phosphatase protein phosphatase 2A (PP2A).

RESULTS

SCYL2 is a Vpu-binding host protein

We initially conducted in vitro protein-protein interaction analysis with full-length HIV-1 Vpu and host proteins. Because Vpu phosphorylation is required for its function, we focused on human protein kinases and related proteins as potential Vpu regulators. We synthesized more than 400 host proteins with a wheat cell-free protein production system (*42*) and screened them for their association with Vpu with the amplified luminescent proximity homogeneous assay (AlphaScreen) (*43*, *44*) (Fig. 1, A and B, and fig. S1). When a relative light unit per cutoff ratio of ≥5000 was used as the threshold, we identified 13 host proteins as potential factors to interact with Vpu that had not been previously known to do so (Fig. 1C). Using gene ontology analysis, we eliminated nuclear proteins relevant to transcriptional regulation or meiosis, enabling us to focus on nine proteins for additional screening (Fig. 1C). To assess the roles of these host proteins in the context of viral replication, we conducted small interfering RNA (siRNA)–based functional analysis of virus particle production. We transfected HeLa cells (which express BST2 endogenously) with siRNAs targeting the nine selected host factors, and then we transfected the cells with an HIV-1 proviral plasmid (pNL4-3). Subsequent measurement of the concentrations of the HIV-1 capsid protein p24 in the culture media by enzyme-linked immunosorbent assay (ELISA) revealed that siRNA specific for SCYL2 caused a substantial increase in viral particle release (Fig. 1D). On the basis of this initial screening, we focused on SCYL2 as a previously uncharacterized Vpu-interacting factor for in-depth functional analysis.

SCYL2 inhibits the particle release of Vpu-positive HIV-1

We next investigated whether SCYL2 affected viral particle release in the presence or absence of either BST2 or Vpu. We transfected HeLa cells with a wild-type or a Vpu-deficient HIV-1 molecular clone (pNL4-3 or pNL4-3ΔVpu) together with a plasmid encoding SCYL2. Viral release assays revealed that in HeLa cells expressing endogenous BST2, the presence of SCYL2 inhibited the release of wild-type HIV-1 particles and increased the amounts of intracellular BST2 (Fig. 2, A and B). Moreover, in cells transfected with pNL4-3ΔVpu, SCYL2 affected neither viral release nor intracellular BST2 abundance (Fig. 2, A and B). We further confirmed that SCYL2 had no observable suppressive effect on viral release in BST2-knockdown HeLa cells (Fig. 2C) or in human embryonic kidney (HEK) 293T cells, which lack endogenous BST2 (Fig. 2D). Moreover, the targeted depletion of endogenous SCYL2 substantially enhanced the release of wild-type virus, but not of Vpu-deficient virus, from cells containing BST2 (Fig. 2, E to G). Together, these results suggested that SCYL2 inhibited the release of viral particles only in the presence of BST2 and Vpu.

SCYL2 inhibits the Vpu-induced reduction in BST2 abundance

Many reports have demonstrated that Vpu enhances viral release by removing BST2 from the cell surface (*11*, *15–20*). To examine whether SCYL2 affected this function of Vpu, we investigated the amounts of cell-surface

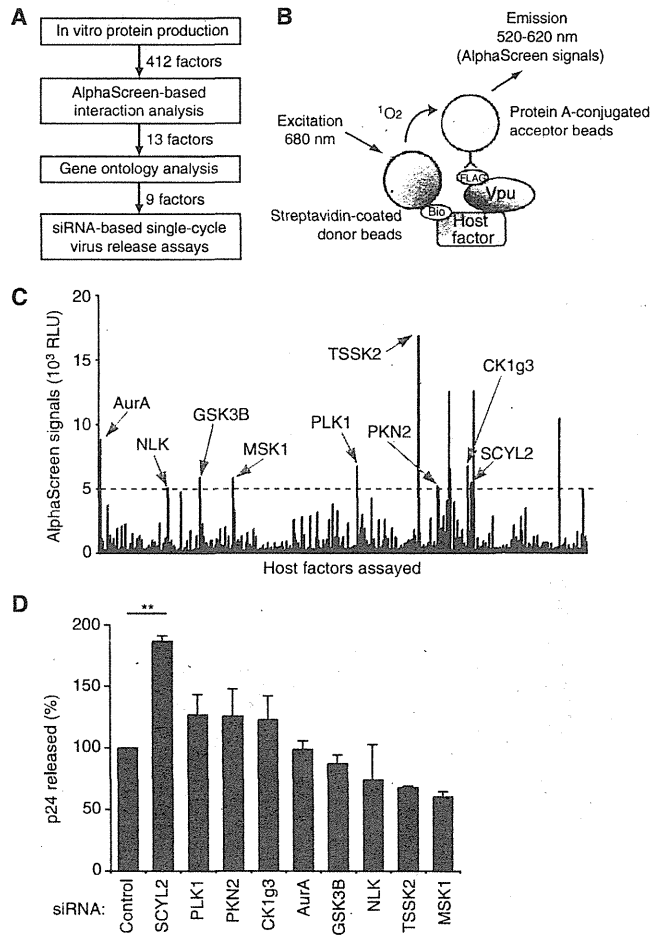

Fig. 1. SCYL2 is a Vpu-binding host protein. (A) Overview of the experimental procedure to detect regulatory factors for HIV-1 Vpu. (B) Schematic representation of the amplified luminescent proximity homogeneous assay used to identify Vpu-interacting proteins. Streptavidin-coated donor beads and anti-FLAG antibody conjugated to protein A acceptor beads were mixed with Vpu and human host proteins. If the two proteins are within 200 nm of each other, AlphaScreen signals are detected. (C) Thirteen proteins with high AlphaScreen signals were processed for further validation by gene ontology analysis. The nine kinases shown were selected as candidate Vpu-interacting host factors. The AlphaScreen was performed in duplicate for each sample. (D) An siRNA-based analysis measuring HIV-1 particle production. HeLa cells were treated with the indicated siRNAs for 24 hours before being transfected with the pNL4-3 molecular clone. Forty-eight hours after transfection, p24 protein in culture supernatants was measured by ELISA. $^{**}P = 0.0030$; $n = 3$ experiments.

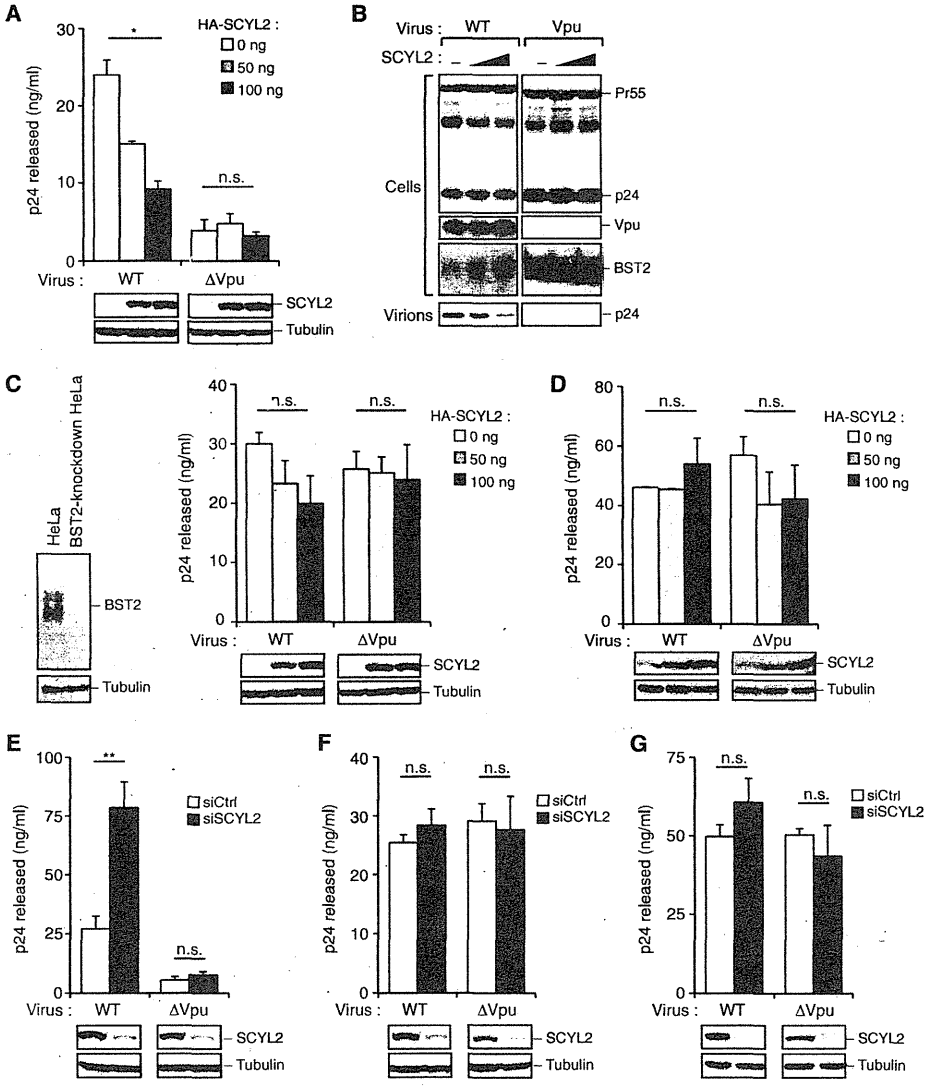

Fig. 2. SCYL2 inhibits the release of particles of Vpu-positive HIV-1. (A and B) Single-cycle virus release analysis of wild-type (WT) or Vpu-deficient HIV-1_{NL4-3}. HeLa cells were cotransfected with the indicated amounts of the SCYL2 expression plasmid together with 100 ng of either pNL4-3 (WT) or pNL4-3ΔVpu (ΔVpu). (A) Forty-eight hours after transfection, culture supernatants were analyzed by ELISA for p24 protein. Blots below the bar graph show the detection of SCYL2 and tubulin by Western blotting. n.s., not significant; $^*P = 0.0206$; $n = 3$ experiments. (B) Cell lysates and supernatants were processed by Western blotting with antibodies against the indicated proteins. (C and D) SCYL2 fails to inhibit viral release from BST2-deficient cells. (C) BST2-knockdown HeLa cells and (D) HEK 293T cells (which have no endogenous BST2) were cotransfected with the indicated amounts of the SCYL2 expression plasmid together with 100 ng of either pNL4-3 or pNL4-3ΔVpu. Forty-eight hours after transfection, culture supernatants were analyzed by p24 ELISA. Western blotting analysis to detect BST2 abundance (C, left) and SCYL2 abundance (C and D, bottom) are shown. n.s., not significant; $n = 3$ experiments. (E to G) SCYL2 depletion enhances viral release from cells containing BST2. Single-cycle virus release analysis of WT or Vpu-deficient HIV-1_{NL4-3} in (E) HeLa cells, (F) BST2-knockdown HeLa cells, and (G) HEK 293T cells. Each cell type was treated with either control (white bars) or SCYL2-specific siRNAs (black bars) for 24 hours before being transfected with either pNL4-3 or pNL4-3ΔVpu (100 ng). Forty-eight hours after transfection, culture supernatants were analyzed by ELISA for p24. Western blotting analysis to detect endogenous SCYL2 abundance is shown at the bottom. n.s., not significant; $^{**}P = 0.0023$; $n = 3$ experiments.

BST2 in HeLa cells expressing Vpu alone or in the presence of SCYL2. Consistent with previous studies, Vpu reduced the abundance of BST2 at the cell surface (Fig. 3A). However, this reduction was less apparent when cells were cotransfected with plasmids encoding both Vpu and SCYL2 (Fig. 3A). Western blotting analysis revealed that the presence of SCYL2 also inhibited the Vpu-mediated degradation of BST2 (Fig. 3B). We next addressed whether SCYL2 affected the anti-BST2 activity of Kaposi's sarcoma–associated herpesvirus (KSHV) K5 protein (*22*, *45*, *46*). Flow cytometric analysis demonstrated that SCYL2 was not able to revert the reduction in the cell-surface abundance of BST2 by KSHV K5 (Fig. 3C). Furthermore, SCYL2 inhibited the ability of Vpu to remove CD4 from the cell surface (Fig. 3D). These results indicated that SCYL2 specifically antagonized the function of Vpu and that this antagonism applied to the effects of Vpu on two cellular targets, CD4 and BST2.

SCYL2 inhibits the phosphorylation of Vpu on Ser^{52} and Ser^{56}

Vpu contains two conserved phosphoacceptor sites (Ser^{52} and Ser^{56}) in its cytoplasmic domain. Phosphorylation of these residues by CKII is required for efficient Vpu function with respect to decreasing the abundances of both BST2 and CD4 (*15*, *23*, *24*, *31*, *32*). We thus speculated that SCYL2 might affect the phosphorylation status of Vpu at Ser^{52} and Ser^{56}. To monitor the extent of Vpu phosphorylation in cells, we used phosphate-affinity polyacrylamide gel electrophoresis (Phos-tag PAGE) (*47*). This method enables the visualization of the phosphorylation status of a protein as a distinct band shift (*48*, *49*). In our Phos-tag PAGE analysis, wild-type Vpu was detected as an upper-shifted band, whereas a mutant Vpu in which Ser^{52} and Ser^{56} were replaced with alanines [Vpu(S52,56A)] was detected as a lower-shifted band, suggesting that the slower-migrating band was as a result of the phosphorylation of Vpu on Ser^{52} and Ser^{56} (Fig. 4A). SCYL2 converted wild-type Vpu into its dephosphorylated state (Fig. 4A). To confirm this observation, we generated a phospho-specific antibody against Ser^{52} and Ser^{56} of Vpu that detects wild-type Vpu but neither the Vpu(S52,56A) mutant nor calf intestinal phosphatase–treated wild-type Vpu (Fig. 4B). We used this antibody for Western blotting analysis and found, as expected, that SCYL2 reduced the extent

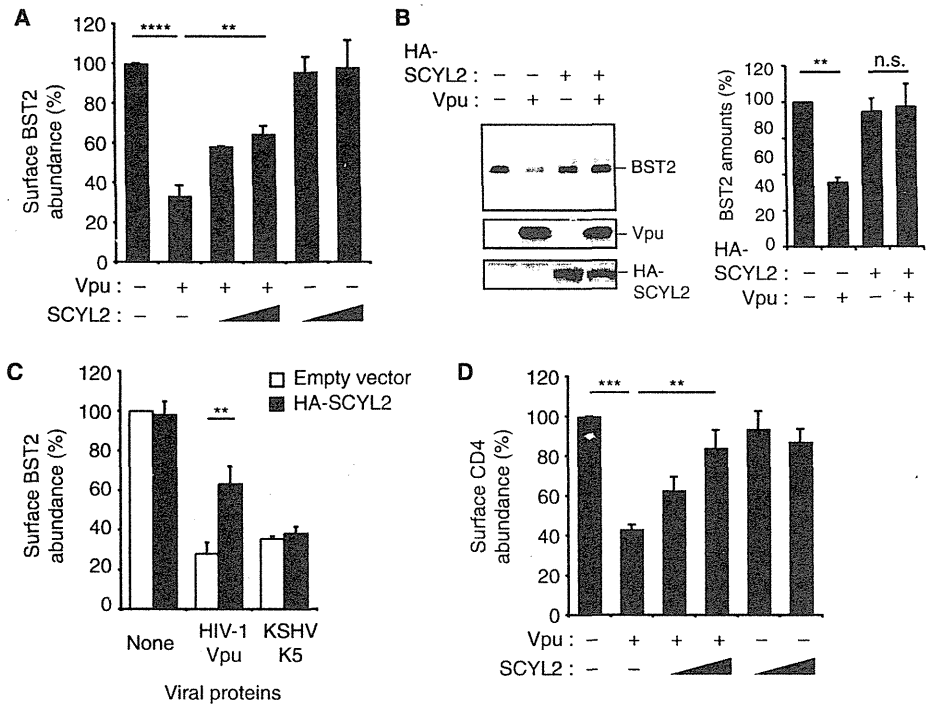

Fig. 3. SCYL2 inhibits the Vpu-induced reduction in BST2 abundance at the cell surface. (A) HeLa cells were transfected with combinations of plasmids encoding Vpu (0 and 100 ng) and hemagglutinin (HA)–SCYL2 (0, 500, and 1000 ng). The cell-surface abundance of BST2 was measured by flow cytometry. ****$P < 0.0001$; **$P = 0.0077$; $n = 3$ experiments. (B) HeLa cells were cotransfected with plasmids encoding Vpu and HA-SCYL2 at a molar ratio of 1:10. Cell lysates were processed for Western blotting analysis with anti-BST2, anti-Vpu, and anti-HA antibodies (left). Representative blots of three experiments are shown. The bar chart indicates the amounts of BST2 as determined by densitometric analysis of Western blots. n.s., not significant; **$P = 0.0020$; $n = 3$ experiments. (C) Selective inhibition of Vpu by SCYL2. HeLa cells were cotransfected with plasmid encoding HA-SCYL2 together with plasmids encoding the indicated viral proteins. After 18 hours, cell-surface BST2 abundance in the presence or absence of HA-SCYL2 was measured by flow cytometry. **$P = 0.0045$; $n = 3$ experiments. (D) SCYL2 inhibits the Vpu-induced downregulation of CD4. H9 cells were transfected with combinations of plasmids encoding Vpu (0 and 100 ng) and HA-SCYL2 (0, 500, and 1000 ng). The cell-surface abundance of CD4 was quantified by flow cytometry. ***$P = 0.0002$; **$P = 0.0083$; $n = 3$ experiments.

of Vpu phosphorylation on Ser^{52} and Ser^{56} (Fig. 4C). Conversely, the targeted depletion of endogenous SCYL2 increased the amounts of phosphorylated Vpu (pVpu) (Fig. 4D). To confirm whether the effect of SCYL2 was mediated by dephosphorylation of Vpu, we treated cells with the CKII inhibitor DRB to suppress the phosphorylation of Vpu on Ser^{52} and Ser^{56}. Treatment with DRB decreased the extent of Vpu phosphorylation, and it inhibited the reduction of cell-surface BST2 abundance by Vpu (fig. S2). Together, these results suggested that SCYL2 inhibited Vpu phosphorylation on Ser^{52} and Ser^{56}, crucial residues for the function of Vpu in the reduction of BST2 abundance, as well as that of CD4.

Both the kinase-like domain and the clathrin-binding domain of SCYL2 are required for its anti-Vpu activity

To verify the association between Vpu and SCYL2 in cells, we next examined the intracellular localization of both proteins by immunofluorescence confocal microscopy. Our results indicated the colocalization of SCYL2 and Vpu in the perinuclear region and cytoplasm (Fig. 5A). We confirmed a direct interaction between SCYL2 and Vpu in vitro with glutathione *S*-transferase (GST) pull-down analysis, which showed that SCYL2 copurified with GST-tagged Vpu (Fig. 5B). We next attempted to determine the binding domain of SCYL2 responsible for its interaction with Vpu in experiments with several truncation mutants of SCYL2 (Fig. 5C). SCYL2 contains an N-terminal kinase-like domain (KLD) and a C-terminal clathrin-binding domain (CBD) (*50–52*). Immunoprecipitation analysis demonstrated that Vpu coprecipitated with either full-length SCYL2 or its two C-terminal truncation mutants, termed SCYL2(N) and SCYL2(ΔCBD), but not with the N-terminal truncation mutant SCYL2(ΔKLD) (Fig. 5C). These results indicated that Vpu interacted with the KLD of SCYL2. We next examined which portions of SCYL2 were important for the dephosphorylation of Vpu and for viral restriction. Our functional analysis demonstrated that SCYL2(ΔKLD) failed to inhibit the activity of Vpu, which was consistent with its inability to bind to Vpu (Fig. 5, D and E). SCYL2(N) and SCYL2(ΔCBD) were also unable to suppress the function of Vpu (Fig. 5, D and E), potentially as a result of their inability to bind to clathrin. These data suggested that both the KLD and CBD of SCYL2 were required for its function.

SCYL2 affects the transport of intracellular proteins through its role in clathrin-mediated membrane trafficking (*51*). The SCYL2 CBD is functionally indispensable because of its association with the clathrin heavy chain (CHC) and the consequent localization of SCYL2 to clathrin-coated vesicles (*51*). To investigate whether clathrin-dependent membrane traffic was necessary for the effects of SCYL2 on Vpu, we performed experiments with cells transfected with CHC-specific siRNA. SCYL2-mediated dephosphorylation of Vpu was inhibited in CHC-depleted cells compared to that in control cells (Fig. 5F). Immunofluorescence analysis further revealed that the depletion of CHC resulted in the diffuse cytoplasmic localization of SCYL2, consistent with a previous report (*51*), and the lack of colocalization of SCYL2 with Vpu (Fig. 5G). These results suggested that clathrin-mediated membrane trafficking is required for the function of SCYL2 as an inhibitor of Vpu.

To address whether the SCYL2-Vpu interaction might be conserved during viral evolution, we investigated the association of SCYL2 with SIV_{GSN} Vpu, an ancient predecessor of HIV-1 Vpu. Amino acid sequence alignment revealed that SIV_{GSN} Vpu lacked the phospho-acceptor sites that correspond to Ser^{52} and Ser^{56} in HIV-1 Vpu (fig. S3A). We found no observable interaction between SIV_{GSN} Vpu and SCYL2 (fig. S3B). Furthermore, cotransfection of cells with plasmids encoding SCYL2 and SIV_{GSN} Vpu did not revert the anti-BST2 activity of SIV_{GSN} Vpu, whereas SCYL2 antagonized the activity of HIV-1 Vpu (fig. S3, C and D). These